GALLAGHER, JACKLYN M., M.S. Isolation of Novel Naphthoquinones from Fungal Strain MSX53507, *Cladorrhinum* sp. (2019)
Directed by Dr. Nicholas H. Oberlies. 47 pp.

This study was conducted as part of an ongoing collaborative project to investigate the chemical diversity of fungi in search of new anticancer drug leads. Fungi have shown to be prolific producers of dynamic secondary metabolites, which exhibit a vast array of physiological activities. In particular, naphthoquinones and their derivatives have long been of interest to medicinal and natural product researchers due to their diverse biological activities such as cytotoxicity, antibacterial, antifungal, antiparasitic, and insecticidal. An established dereplication protocol for screening and prioritization of fungal samples for cytotoxicity, indicated that the biological activity of MSX53507 was not attributable to any compounds (new or known) previously isolated and identified in our research laboratory. Bioactivity-guided fractionation, the primary methodology in our laboratory in which results can take weeks, was conducted solely for screening and prioritization of fractions for further investigation. Preliminary work yielded compounds which encompass an easily identifiable feature in ^{1}H-NMR spectroscopy that is characteristic to this class of compounds. Employing a proton-NMR guided fractionation methodology for purification of biologically active fractions, led to the isolation of four new naphthoquinone analogues (**1**, **3**, and **6-7**), two known compounds (**4-5**) and a naphthoquinone previously misidentified in the literature (**2**). Naphthoquinone's broad spectrum of biological activity led us to test compounds **2**, **5**, and **6** against *Staphylococcus aureus* (ATCC 35667) and a clinically relevant methicillin-resistant *S.*

aureus strain (MRSA) where **5** was the most active with minimum inhibitory concentrations (MICs) of 2.3 μg/mL and 16.0 μg/mL, respectively.

ISOLATION OF NOVEL NAPHTHOQUINONES FROM FUNGAL STRAIN MSX53507, *CLADORRHINUM* SP.

by

Jacklyn M. Gallagher

A Thesis Submitted to
the Faculty of The Graduate School at
The University of North Carolina at Greensboro
in Partial Fulfillment
of the Requirements for the Degree
Master of Science

Greensboro
2019

Approved by

_____
Committee Chair

In Loving Memory of

John F. Gallagher

APPROVAL PAGE

This thesis, written by Jacklyn M. Gallagher, has been approved by the following committee of the Faculty of The Graduate School at The University of North Carolina at Greensboro.

Committee Chair _____
Nicholas H. Oberlies

Committee Members _____
Ethan W. Taylor

_____
Ramji K. Bhandari

_____
Date of Acceptance by Committee

_____
Date of Final Oral Examination

ACKNOWLEDGEMENTS

First I want to thank my advisor, Dr. Nicholas H. Oberlies, for being a wonderful mentor and supporter to the research I have conducted while in the laboratory. Your support, motivation and advice pushed me to step outside of my comfort zone and not only succeed at accomplishing things that I thought were only a dream and beyond my knowledge, such as the Yale workshop, but also built confidence. I will always take with me your advice that I won't know if I don't try, and not trying is a no, so there is no loss in trying. Lastly, I am beyond grateful for the patience, kindness, understanding and invaluable time you afforded me to spend with family when it was most important.

To my mentor, Dr. José Rivera-Chávez, thank you for providing me the foundation to succeed. Your advice, support, patience and guidance allowed me to become the researcher I am today.

I would like to thank my committee members Dr. Ramji Bhandari and Dr. Ethan Taylor for their valuable input, advice and thought provoking conversations for the work I have done and the future work I hope to embark on.

I am extremely grateful to my parents. There are not enough words to describe how thankful I am for all your support, patience, advice and love. Thank you for believing in me and also putting up with all the crazy hours in lab, or at the other jobs. Also, great thanks to my fiancé and his family for their support, kindness and love.

I would like to extend my sincere thanks to Joseph Egan for not only noticing my curiosity in chemistry, but also recommending I conduct research in the Oberlies Lab

based on my skill set that you observed. Not only have you been a great mentor, but you have also become a great friend, and I am grateful for all the support, suggestions, and last minute proof-reading of various proposals.

I am grateful to Tyler Graf for all of the advice and assistance throughout the years. I never imagined that I would ever try to troubleshoot mechanical issues on my own before calling for help. Also, a special thank you to Dr. Huzefa Raja for teaching me about fungi, and giving me the opportunity to work on many different types of projects during my time as an undergraduate student, and research assistant.

Many thanks to both Dr. Diana Kao and Zeinab Al Subeh for your compassion, concern, emotional support and giving me strength when a family member was ill.

Special thanks to the rest of the Oberlies Lab members both past and present. In particular Sonya Knowles and Dr. Laura Flores Bocanegra for assistance and guidance in the laboratory, Allison Wright and ZuZu Faye for help with enzyme mechanisms and Dr. Noemi Paguigan, Dr. Soumia Amrine and Franklin Turner for always smiling and laughing.

I am also grateful to all my friends who stood by me and supported me through this journey, in particular Sara, Allison and Mike.

I would like to recognize the Department of Chemistry and Biochemistry at UNCG for the financial support awarded to me through a teaching assistantship. Also, many thanks to all the faculty in the department for providing such a wonderful, friendly and supportive environment to conduct research.

TABLE OF CONTENTS

Page

LIST OF TABLES

Page

LIST OF FIGURES

Page

CHAPTER I

INTRODUCTION

The International Agency for Research on Cancer (IARC) projects that by 2030 there will be 21.7 million new cancer diagnoses and 13 million cancer deaths.[1] Cancer, the uncontrolled growth of abnormal cells, is ranked as the second leading cause of death globally with about 1 in 6 people worldwide dying from some form of cancer.[1] Breast cancer accounts for more than 25% of new cancer diagnoses in women, and resulted in over two million new diagnoses and a little less than 630,000 deaths in 2018 alone.[1] The financial impact of cancer is also astounding, with estimated costs in Europe for 2014 around $110 billion and about $80.2 billion in the United states for 2015.[1] While the causes of cancer remain largely unknown, the need for new chemotherapeutic agents is well known since there is no drug capable of treating all cancers.

The World Health Organization (WHO) reports lower respiratory tract infections as the leading cause of death in low income countries and the overall fourth leading cause of death globally (top ranked communicable disease).[2] The ESKAPE pathogens (*Enterococcus faecium*, *Staphylococcus aureus*, *Klebsiella pneumoniae*, *Acinetobacter baumannii*, *Pseudomonas aeruginosa*, and *Enterobacter* sp.) are common culprits for respiratory infections.[3] A recent study in children in China found that the level of antibiotic resistance was directly associated with the antibiotics used in the clinic and that Methicillin-Resistant *Staphylococcus aureus* (MRSA) and Methicillin-Sensitive

Staphylococcus aureus (MSSA) were most commonly isolated in infants less than three months, while *K. pneumoniae* (including Extended Spectrum β-Lactamase [ESBLs] resistant *K. pneumoniae*) was most commonly isolated from infants less than one month in age.[4] A different study, not limited to children, found the most commonly isolated pathogen from respiratory specimens was *Klebsiella* ssp (25.20%) while the third most common pathogen was *S. aureus* (19.89%).[5] Additionally, they observed that bacterial isolates had high rates of resistance to drugs such as Co-trimoxazole (80%), Ampicillin sulbactam (72.3%), Cefotaxime (68.8%) and Tetracycline (66.9%), while low resistance was found to Amikacin (4.6%) and Levofloxacin (8.5%).[5] The over-prescribing and misuse of antibiotics globally is considered a direct cause of increased antibiotic resistance due to the medications selective pressure on antimicrobials which then leads to increased resistance.[5] Increased use of over the counter antibiotics, in addition to half of the dispensed antibiotics not being essential, generates not only antibacterial resistance at the individual level, but can also threaten the entire community.[5]

Natural sources have yielded a wide array of compounds leading to advancements in medicine. Approximately 50% of new drugs approved by the FDA between 1981 and 2014 came from either a natural product, a natural product mimic (or modification), or a natural product pharmacophore.[6] Several billion years of evolution has generated an immerse diversity within nature, with an estimated 250,000 different species of plants, up to 30 million species of insects, 2.2-3.8 million species of fungi and around 1.5 million species of algae and prokaryotes currently in existence.[7, 8] Coexistence and interactions between species, can affect or alter the secondary metabolites produced, making the

chemical diversity enormously vast.[8] This can be best seen with endophytic relationships, and even demonstrated in co-culture experiments with fungi.[9, 10] A recent review of natural products reported that 85 of the 175 small molecules approved for cancer treatments between the 1940s to the end of 2014 were either a natural product or directly derived from one of them.[6]

The fungal kingdom is not only the second most diverse, but also highly underexplored with only 3 to 8% identified.[11] Furthermore, only 5% (about 14,000) of the 250,000 compounds described from nature, come from fungi.[9] Despite these numbers, fungi have shown to be prolific producers of dynamic secondary metabolites, which exhibit diverse physiological activities. They have shown to be promising sources for potential drug leads, with life-saving drugs such as β-lactam antibiotics (includes Penicillin G), statins (cholesterol-lowering drugs) and immunosuppressants coming from fungi.[9] Most medicines of fungal origin come from the phylum Ascomycota, the largest of the eight fungal phyla, with approximately 90,000 species described.[12] While some ascomycetes have had positive attributes and impacts such as in medicine, and consumables, including delicacies (truffles) and yeasts (used in fermentation of alcohols), others have been pathogenic to plants and animals.[12] Currently, there are less than twenty reported *Cladorrhinum* species (per Mycobank.org), in which most are either endophytes found in roots or saprotrophs found on dung, plant material or leaf litter.[13-15] Even though some species are being investigated as potential biocontrol agents against fungal phytopathogens (*Rhizoctonia solani* – "root rot") and in general, species from *Cladorrhinum* are considered a group of "fundamental importance for agriculture and

livestock", at least one species has been involved in opportunistic infections in both animals and humans.[13-15] The biological activity of secondary metabolites isolated from *Cladorrhinum* spp. is not limited to just promoting plant growth, having biocontrol potentials, or opportunistic effects, but has also produced compounds (MPC1001, and MPC1001B-D) that exhibited antiproliferative activities against human prostate cancer cell line DU145 with IC_{50} values ranging between 9.3 nM and 39 nM.[14, 16]

Naphthoquinones and their derivatives have long been of interest to medicinal and natural product researchers.[17, 18] This class of compounds has promising potential for therapeutic leads due to their wide array of biological activities such as cytotoxicity, antibacterial, antifungal, anti-parasitic, insecticidal, anti-tubercular, anti-malarial, anti-inflammatory, and anti-HIV to name a few.[17-31] These activities can be attributed to mainly two groups based upon their molecular mechanisms in cells.[17] The first mechanism is via introduction of oxidative stress by generating reactive oxygen species and the second is by a non-oxidative mechanism via interactions directly with traditional therapeutic targets.[17] Naturally occurring naphthoquinones and their derivatives have been isolated from many different fungi, across a variety of genera.[17, 25, 27, 30, 31]

The chemical diversity and biological potential of secondary metabolites from fungi is highly underexplored with only approximately 120,000 species of fungi (3-8%) within the 2.2-3.8 million that is estimated within the kingdom being identified. Our laboratory's research goal is to investigate the biological potential of secondary metabolites produced by fungi to not only expand the chemical space, but also to look for new compounds which are cytotoxic or encompass a structural core for use in

development of therapeutic leads focusing primarily on cancer drug leads. The first aim of this research is to use a previously established eight step protocol for isolation of novel compounds, or compounds which have not previously been isolated by our laboratory that are cytotoxic (**Figure 1**). First the fungi are grown on solid media and then extracted with organic solvents. The extract is screened against three cancer cell lines (MDA-MB-435, MDA-MB-231, and OVCAR3). Extracts that are cytotoxic are then subjected to an established dereplication protocol using UPLC-MS/MS, where they are screened against an in-house library of all the compounds that have been isolated in our laboratory which are known to be cytotoxic. This is to avoid the re-isolation of known compounds, and to prioritize fungal samples for investigation. The highest priority for further investigation is assigned to a fungal sample that not only exhibits good cytotoxicity, but also one who's biological activity isn't attributable to a cytotoxic compound previously isolated in our laboratory. Once these steps have been accomplished, the extract is then further fractionated using liquid chromatography. These fractions are then again sent for screening against the same cancer cell lines, and only the active fractions are worked with further. The active fractions then undergo further separation and purification using liquid chromatography to obtain pure compounds. The second aim of this project is to determine which isolated compound is responsible for the biological activity observed during cytotoxicity screening and to determine the structures of the new compounds. The compound's structures are then elucidated using a set of spectroscopic and spectrometric techniques, and the pure compounds (+95% purity) are then tested again for their biological activity. While bioactivity-guided fractionation is the primary methodology

employed in our laboratory, it can take weeks to obtain the results. Thus, this part of the method was conducted solely for screening and prioritization of fractions for further investigation. Results from the preliminary screening of MSX53507 against the three cancer cell lines determined the extract and some fractions were cytotoxic. This data coupled with the results from dereplication, indicated that the biological activity of MSX53507 was not attributable to any compounds (new or known) previously isolated and identified in our research laboratory. Preliminary work yielded compounds which encompass an easily identifiable feature, a chelated peak, in ^{1}H-NMR spectroscopy that is characteristic to this class of compounds. Therefore, a proton-NMR guided fractionation methodology for purification of biologically active fractions was employed for this project.

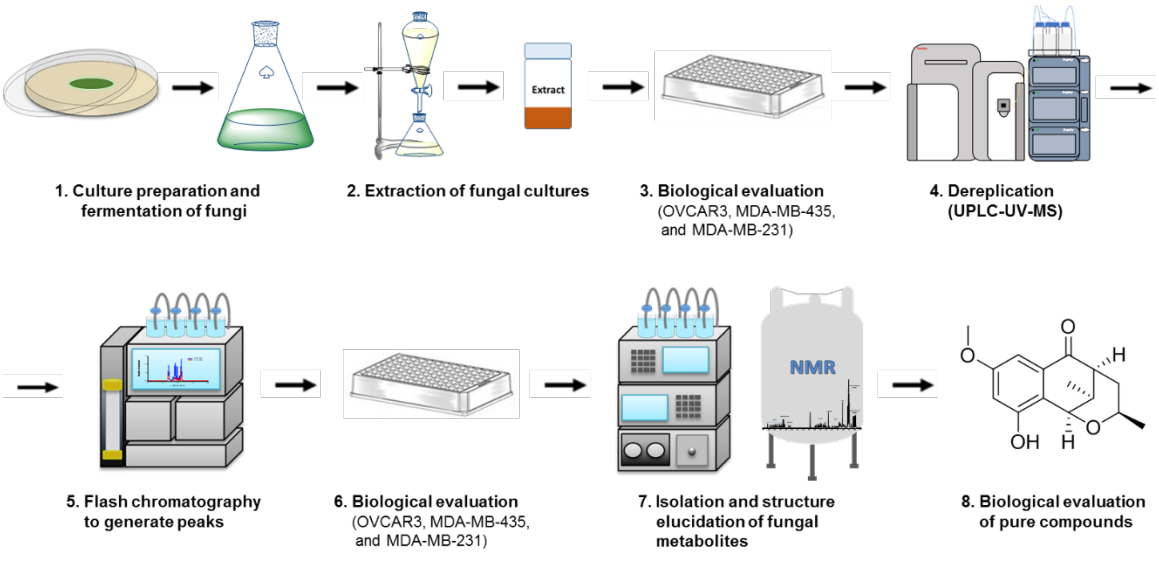

Figure 1. Experimental Protocol Depicting the Previously Established General Methodology for Extraction and Isolation of Bioactive Compounds.

This thesis contains two chapters detailing the isolation and elucidation of novel and known biologically active secondary metabolites from fungal strain MSX53507, as well as a conclusion chapter. This work was conducted as part of an ongoing collaborative project to uncover new anti-cancer drug leads. The results from preliminary screening of fractions against cancer cell lines MDA-MB-435 (melanoma), MDA-MB-231 (breast), and OVCAR3 (ovarian) in combination with an established dereplication protocol, suggested further investigation of MSX53507 was needed. Proton-guided fractionation led to the isolation and characterization of seven naphthoquinone analogues, of which four are entirely new to the literature. Two are an unprecedented, dimeric, 6'-12 head-to-tail binding of some of the isolated monomeric naphthoquinones, while another new compound contains a bridged eight-member oxocine-one ring system in which the bridge creates two six-membered rings. Naphthoquinone's broad spectrum of biological activity led us to test some of the compounds against *Staphylococcus aureus* (ATCC 35667) and a clinically relevant methicillin-resistant *S. aureus* strain (MRSA). Interestingly, fungal strain MSX53507 utilizes the same building block to generate some of the new chemotypes identified, and ultimately showcases the broad and divergent biosynthetic pathways of fungi.

CHAPTER II

RESULTS AND DISCUSSION

Isolation and Structure Elucidation

Previously, fungal strain MSX53507 was extracted, fractionated into four peaks, and screened against three cancer cell lines: melanoma (MDA-MB-435), breast (MDA-MB-231), and ovarian (OVCAR3). The results from an established dereplication protocol along with the preliminary cytotoxicity data, led to the isolation of naphthoquinone analogues (**2**, **3** and **5**).[32, 33] This information, in addition to a limited availability of material, led to the work described here within; isolation of biologically active secondary metabolites produced by the fungus MSX53507.

Two large-scale cultures of MSX53507 were ordered from our collaborator, Mycosynthetix. However, due to the morphological diversities of this fungus, three large scale cultures that were grown on rice were obtained (one light, and two dark). The light colored culture was extracted separately from the two dark growths using established laboratory protocols which was performed in triplicate to obtain the maximum amount of organic extract (**Figure 1**).[11] The obtained extracts were then partitioned with organic solvents, and the resultant organic fraction was defatted. These extracts were then fractionated using flash chromatography, and purified further using preparative, semi-preparative, and analytical HPLC to obtain four new compounds (**1**, **3**, and **6**-**7**), two known compounds (6-deoxybostrycoidin (**4**) and 6-deoxyfusarubin (**5**)), and one which

we intend to correct the literature and will spectroscopically describe for the first time (**2**) (**Figure 2**).

Flash chromatography of the light extract was pooled into nineteen fractions, in which fraction 8 was further purified to obtain compound **1**. To the best of my knowledge, this is the first report of an oxocine-one core, formed from a monomeric unit, isolated from fungi.[34, 35] Flash chromatography of the dark extract yielded 23 fractions. Compound **7** was isolated from HPLC purification of fraction 11. Fraction 10, was subjected again to flash chromatography, using a different solvent system, in which ten fractions were obtained. From these ten fractions, compound **6** was isolated from fraction 7, while fraction 5 was further purified to obtain compounds **2-5** (**Figure 2**).

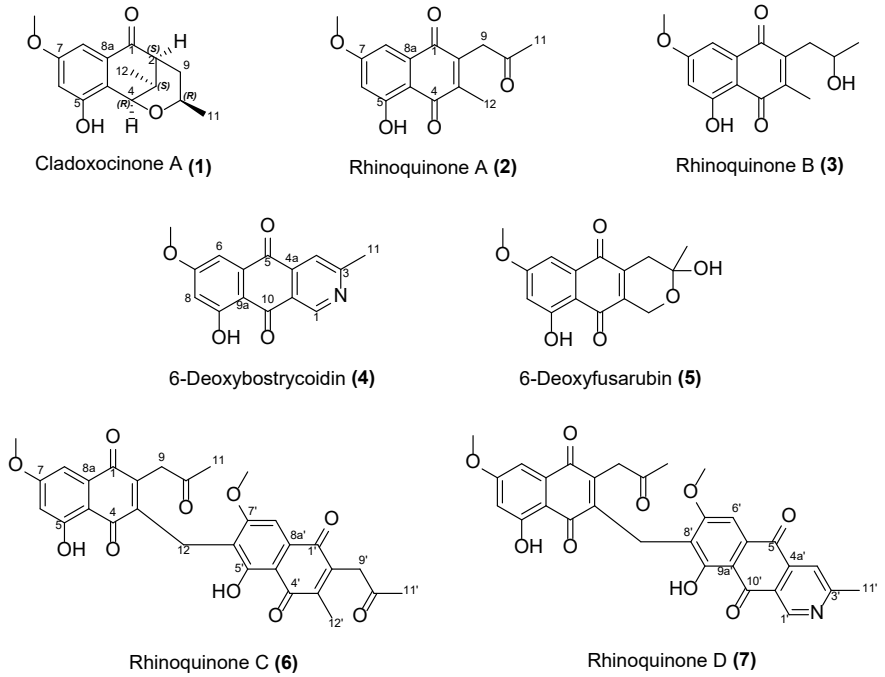

Figure 2. Structures of Compounds **1-7**.

The structures of the isolated compounds were established using spectroscopic and spectrometric data. The structure of **2** was confirmed with X-Ray crystallography. While the known compounds compared favorably to the literature, there were some discrepancies observed in the spectroscopic data. The relative configuration of **1** was assigned from the observed ^{1}H NMR coupling constants.

Compounds **4** and **5** were first described almost 30 years ago, and their parent compounds, bostrycoidin and fusarubin, were first isolated between 60 to 70 years ago (Dictionary of Natural Products).[19, 36] The parent compounds are both 5,8-dihydroxy-1,4-naphthoquinones. These two alcohols allow for tautomerization to occur. Due to the aromaticity in the rings, both ketones must tautomerize to the alcohol. Therefore, you cannot have two rings with one ketone and alcohol on each and will always have one ring that contains both ketones and the other will have both alcohols. Thus, the tautomer of the naphthoquinone may be what is reported in the literature, which is the case for bostrycoidin and fusarubin. The early NMR data for both of these three-ring structures is reported with the alcohols on the middle ring, and ketones on the outside ring. This structural change will also cause the signals observed in NMR spectra to change, ultimately making the spectra incomparable if you have the tautomer. However, it should be noted, the absence of one of the hydroxy groups would prevent tautomerization.

Compound **1** was isolated as a white amorphous solid, with its molecular formula as $C_{15}H_{18}O_4$ from HRESIMS data ($[M+H]^+$ *m/z* = 263.1274, calculated *m/z* = 263.1278 for $C_{15}H_{19}O_4$, Δ -1.5 ppm) with an index of hydrogen deficiency of seven. Analysis of the ^{1}H, ^{13}C (**Appendix Figure A1**), and edited-HSQC data showed signals for two aromatic

protons (δ_H/δ_C 6.73 (d, J = 2.5)/109.6 and δ_H/δ_C 7.16 (d, J = 2.5)/101.5), one methoxy group (δ_H/δ_C 3.84/55.8), two methyls (δ_H/δ_C 1.10 (d, J = 6.1)/21.8; δ_H/δ_C 0.89(d, J = 7.2)/16.8), one methylene which exhibited geminal splitting of the protons ($\delta_{H\text{-}\alpha}$ 1.86 (ddd, J = 13.6, 3.1, 3.1), $\delta_{H\text{-}\beta}$ 1.77 (ddd, J = 13.6, 12.3, 4.8)/δ_C 38.7), and four methine protons (δ_H/δ_C 2.49 (qdd, J = 7.2, 3.3, 2.6)/37.4; δ_H/δ_C 2.74 (ddd, J = 4.8, 2.6, 2.6, 2.6)/48.2; δ_H/δ_C 3.51 (ddq, J = 11.9, 5.9, 3.2)/63.3 and δ_H/δ_C 5.03 (dd, J = 3.2, 1.4)/69.3) as well as five non-protonated carbons, including two non-protonated (δ_C 155.9, 160.7), two aromatic (δ_C 116.7, 135.7), and one ketone in the oxocine-one ring (δ_C 200.6) (**Table 1**). Examination of the HMBC spectrum showed key correlations from H-6 to C-4a, C-5, C-7 and C-8, 7-OCH_3 to C-6, C-7 and C-8, H-8 to C-1, C-4a, C-6, C-7, and C-8a, H-3 to C-1, C-2, C-4, C-4a and C-12, H-4 to C-2, C-3, C-4a, C-5, C-8a and C-10, H_α-9 to C-1, C-2 and C-3, H_β-9 to C-1, C-2, C-3, C-10 and C-11, H_3-11 to C-9 and C-10 and H_3-12 to C-2, C-3 and C-4 and support the structure shown in **Figure 2**. The relative configuration was derived from the coupling constants shown in **Figure 3** and assigned the trivial name Cladoxocinone A.

Table 1. ^{1}H (700 MHz) and ^{13}C (175 MHz) NMR Data for Compound **1**, Recorded in $CDCl_3$ with *J* (Hz) Values Color Coded to Correspond with Figure 3.

Position	δ_C	Type	δ_H	Multiplicity, *J* (Hz)
1	200.6	C		
2	48.2	CH	2.74	ddd[a], 4.8, 2.6, 2.6, 2.6
3	37.4	CH	2.49	qdd, 7.2, 3.3, 2.6
4	69.3	CH	5.03	dd, 3.2, 1.4
4a	116.7	C		
5	155.9	C		
6	109.6	CH	6.73	d, 2.5
7	160.7	C		
8	101.5	CH	7.16	d, 2.5
8a	135.7	C		
9	38.7	CH_2	α 1.86	ddd[b], 13.6, 3.1, 3.1
			β 1.77	ddd, 13.6, 12.3, 4.8
10	63.3	CH	3.51	ddq[c], 11.9, 5.9, 3.2
11	21.8	CH_3	1.10	d, 6.1
12	16.8	CH_3	0.89	d, 7.2
5-OH			5.64	
7-OCH_3	55.8	CH_3	3.84	

Note: [a] dq was observed multiplicity due to overlapping *J*-values (4.8, 2.6, 2.6, 2.6)
[b] dt was observed multiplicity due to overlapping *J*-values (13.6, 3.1, 3.1)
[c] dtq was observed multiplicity due to overlapping *J*-values (11.9, 6.0, 3.2)

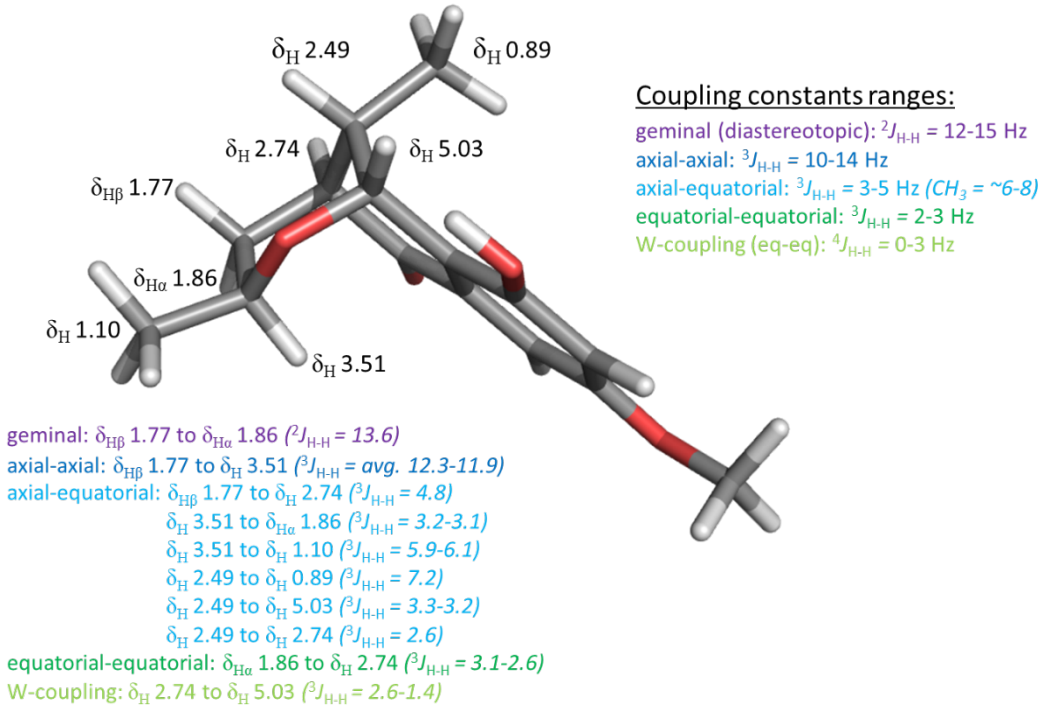

Figure 3. Detailed Analysis of Select Proton's Coupling Constants Used for Proposal of the Relative Configuration and Conformation of Compound **1**.

While the structure for compound **2** has been previously reported in the literature and referenced incorrectly as 2-acetonyl-3-methyl-5-hydroxy-7-methoxy-naphthazarin (javanicin)[18, 25, 37], we present for the first time all spectroscopic data showing it is not javanicin[38] or the tautomer and assign the trivial name rhinoquinone A. Compound **2** was isolated as a golden-yellow amorphous solid, that formed thin golden-orange needle-like crystals from an approximate 1:1 $CHCl_3$:MeOH solution under nitrogen drying lines. The molecular formula was determined as $C_{15}H_{14}O_5$ from HRESIMS data ($[M+H]^+$ *m/z* = 275.0910, calculated *m/z* = 275.0914 for $C_{15}H_{15}O_5$, Δ -1.3 ppm) with nine degrees of unsaturation. Analysis of the ^1H, ^{13}C (**Figure A2**), and edited-HSQC data showed signals

for two aromatic protons (δ_H/δ_C 6.63 (d, J = 2.5)/106.1; δ_H/δ_C 7.15 (d, J = 2.5)/107.9), one methoxy group (δ_H/δ_C 3.89/56.1), one chelated proton (δ_H 12.34), two methyls (δ_H/δ_C 2.31/30.4; δ_H/δ_C 2.11/12.8), one methylene (δ_H/δ_C 3.77/41.8), as well as nine non-protonated carbons, including two non-protonated (δ_C 164.3, 165.9), two aromatic (δ_C 109.7, 133.3), two olefinic (δ_C 141.0, 146.3), two ketones in the *p*-quinone ring (δ_C 183.4, 188.1), and one aliphatic ketone (δ_C 203.4) (**Table 2**). Examination of the HMBC spectrum showed key correlations often seen with 1,4-naphthoquinones, allowing for the establishment of structure **2** as shown in **Figure 2**. In particular, the correlations from 5-OH to C-4a, C-5 and C-6, H-6 to C-4a, C-5, C-7, and C-8, 7-OCH_3 to C-7, and H-8 to C-1, C-4a, C-6, C-7, and C-8a support the 1,4-naphthoquinone core, along with H_3-12 to C-1, C-2, C-3, C-4, C-9, and C-10, and H_2-9 to C-1, C-2, C-3 and C-10 supporting both the *p*-quinone ring and chain, while H_3-11 to C-9 and C-10 established the acetonyl chain. The structure was confirmed via X-ray crystal diffraction (**Figure 4**), and the data will be deposited to Cambridge Crystallographic Data Centre (CCDC) and an accession number assigned at that time. Comparison of the X-ray crystal diffraction data of both javanicin[27] and rhinoquinone A, depicts that absence of a hydroxy moiety at the C-8 position in compound **2** would prevent tautomerization of the diketones, and establishes these as two different compounds.

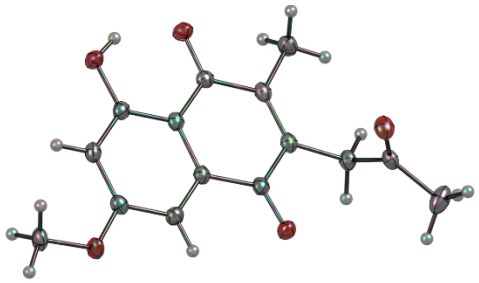

Figure 4. X-Ray Crystallographic Structure of Compound **2**.

Table 2. ^{1}H (400 MHz) and ^{13}C (100 MHz) NMR Data for Compound **2**, Recorded in $CDCl_3$.

Position	δ_C	Type	δ_H	Mult, *J* (Hz)
1	183.4	C		
2	141.0	C		
3	146.3	C		
4	188.1	C		
4a	109.7	C		
5	164.3	C		
6	106.1	CH	6.63	d, 2.5
7	165.9	C		
8	107.9	CH	7.15	d, 2.5
8a	133.3	C		
9	41.8	CH_2	3.77	s
10	203.4	C		
11	30.4	CH_3	2.31	s
12	12.8	CH_3	2.11	s
5-OH			12.34	s
7-OCH_3	56.1	CH_3	3.89	s

Compound **3** was obtained as a golden-yellow amorphous solid, and its molecular formula was determined as $C_{15}H_{16}O_5$ based upon the HRESIMS data ($[M+H]^+$ *m/z* = 277.1066, calculated *m/z* = 277.1071 for $C_{15}H_{17}O_5$, Δ -1.6 ppm) indicating an index of hydrogen deficiency of eight. The ^{1}H, ^{13}C (**Figure A3**), edited-HSQC, and HMBC data is remarkably similar to **2**, supporting the 1,4-naphthoquinone core. However, the C-9

methylene and C-11 methyl were slightly more shielded (δ_H/δ_C 2.80/36.7 and δ_H/δ_C 1.31/24.3 respectively) (**Table 3**). The presence of two additional signals in the ^1H spectra and the decrease in degrees of unsaturation, support the molecular formula and are attributed to the reduction of the aliphatic ketone. Examination of splitting patterns in the chain, signals for the oxymethine (δ_H/δ_C 4.04 (m)/67.9), and 10-OH (δ_H 1.86 (d, J = 5.3) in addition to key HMBC correlations from 10-OH to C-9, C-10 and C-11, support the planar structure shown in **Figure 2** and is given the trivial name rhinoquinone B.

Table 3. ^1H (500 MHz) and ^{13}C (125 MHz) NMR Data for Compound **3**, Recorded in $CDCl_3$.

Position	δ_C	Type	δ_H	Mult, J (Hz)
1	185.1	C		
2	145.6	C		
3	144.6	C		
4	188.5	C		
4a	109.6	C		
5	164.1	C		
6	106.1	CH	6.63	d, 2.5
7	165.8	C		
8	107.8	CH	7.17	d, 2.5
8a	133.6	C		
9	36.7	CH_2	2.80	m
10	67.9	CH	4.04	m
11	24.3	CH_3	1.31	d, 6.2
12	12.9	CH_3	2.22	s
5-OH			12.39	
7-OCH_3	56.1	CH_3	3.90	s
10-OH			1.86	d, 5.3

Compound **4**, isolated as a yellow amorphous powder, was determined to be the known compound 6-deoxybostrycoidin. The molecular formula was $C_{15}H_{11}NO_4$ according to the HRESIMS data ($[M+H]^+$ m/z = 270.0756, calculated m/z = 270.0761 for

$C_{15}H_{12}NO_4$, Δ -1.8 ppm), with eleven degrees of unsaturation. The ^{1}H-NMR spectra (**Figure A4**) was mostly in agreement with the reported data, but minor variations in the signals was observed with the largest variance being 0.06 ppm for the aromatic proton H-6 (δ_H experimental 7.38, δ_H reported 7.32) (**Table 4**).[39] Preliminary assignment of the ^{13}C signals from the 2D-NMR data (edited-HSQC and HMBC) seem to be in alignment with the reported except for C-6 and C-8 being reported as δ_C 107.4 and δ_C 108.1 respectively.[39] However, we assigned these signals in the opposite manner due to the H-8 proton being more shielded from its adjacent oxygenated substituents, which also aligned with the predicted ^{13}C NMR data that was calculated using ACD laboratories NMR predictor software.

Table 4. ^{1}H (400 MHz) and ^{13}C (100 MHz) NMR Data for Compound **4**, Recorded in $CDCl_3$.

Position	δ_C Obtained	Type	δ_H	Mult, *J* (Hz)	δ_C Reported	δ_C Calculated
1	*149.4	CH	9.44	s	149.1	149.3
3	*166.0	C			165.6	164.1
4	*118.8	CH	7.88	s	118.5	118.1
4a	*138.8	C			134.6	137.5
5	*182.4	C			185	183.6
5a		C			138.7	134.4
6	*108.4	CH	7.38	d, 2.4	107.4	108.1
7	*167.1	C			165.9	165.4
8	*107.6	CH	6.77	d, 2.4	108.1	106.7
9	*166.0	C			166.54	164.7
9a	*111.1	C			110.5	112.8
10	*186.3	C			182	187.0
10a	*124.4	C			124	123.9
3-CH_3	*25.4	CH_3	2.78	s	25.3	24.7
7-OCH_3	*56.3	CH_3	3.95	s	56.1	56.3
9-OH			12.80	s		

**Signals derived from 2D NMR Data, edited-HSQC and HMBC.*

Compound **5**, also a known compound, (6-deoxyfusarubin / 9-desmethylherbarine), was initially isolated as a yellow amorphous powder, but crystallizes into dark orange-brown crystals from $(CD_3)_2SO$ under nitrogen drying lines.[19, 22, 40] The molecular formula was $C_{15}H_{14}O_6$ on the basis of the HRESIMS data ($[M+H]^+$ *m/z* = 291.0858, calculated *m/z* = 291.0863 for $C_{15}H_{15}O_6$, Δ -1.8 ppm), with an index of hydrogen deficiency of nine. Interestingly, when comparing the 1D-NMR spectra (**Table 5** and **Figure A5**) obtained in $(CD_3)_2SO$ to two different reports of **5** by Parisot et al., it is observed they have assigned their ^{1}H-NMR signals differently between the two reports, along with reported carbon signals of an analogue similar to compound **5**.[19, 40] Recently, Chowdhury et al., reported the compound as new by establishing the relative configuration from analysis of NOESY correlations and renamed it 9-desmethylherbarine.[22] Comparison of the reported 1D-NMR data and obtained (both in $CDCl_3$) aligned much more closely. Small differences were observed, particularly with the signals most affected by the stereocenter at C-3.[22] Thus the obtained data was in alignment with the reported data and the planar structure in **Figure 2** is supported.

Table 5. ^{1}H (500 MHz) and ^{13}C (125 MHz) NMR Data for Compound **5**, Recorded in $(CD_3)_2SO$.

Position	δ_C	Type	δ_H	Mult, *J* (Hz)
1	57.2	CH_2	4.54	m
3	93.8	C		
4	33.2	CH_2	2.59, 2.46	m
4a	142.0	C		
5	182.9	C		
5a	133.8	C		
6	107.9	CH	7.04	d, 2.4
7	166.1	C		
8	106.3	CH	6.83	d, 2.4
9	164.0	C		
9a	109.1	C		
10	186.8	C		
10a	140.9	C		
3-CH_3	28.8	CH_3	1.46	s
3-OH			6.12	m
9-OH			12.05	s
7-OCH_3	56.9	CH_3	3.91	s

Compound **6** was isolated as a bright yellow amorphous solid. Its molecular formula was established as $C_{30}H_{26}O_{10}$ from the HRESIMS data ($[M+H]^+$ *m/z* = 547.1590, calculated *m/z* = 547.1599 for $C_{30}H_{27}O_{10}$, Δ -1.6 ppm) with an index of hydrogen deficiency of eighteen. The ^{1}H data showed a spectrum strikingly similar to compound **2**, with an initial appearance of each signal being duplicated with two methoxys, two chelated protons, and two methylenes. However, key differences observed in the 1D-NMR spectra (**Figure A6**) was the presence of only three methyl units (instead of four if duplicated), three aromatic protons with one being a singlet instead of a doublet with a meta-coupling constant as seen previously, and an additional methylene that was confirmed with edited-HSQC. Analysis of the HMBC data determined that the C-12

methyl observed in **2**, was now a methylene unit (δ_H/δ_C 4.01 (s)/19.9), connected to a second unit of rhinoquinone A at the C-6' position (δ_C 120.1) and also supported by the observed singlet for H-8' (δ_H/δ_C 7.13/102.9). (**Table 6**). The key HMBC correlations confirming the structure (**Figure 2**) were H_2-12 to C-2, C-3, C-4, C-5', C-6' and C-7', along with the ones previously described in **2** supporting the naphthoquinone core. We have assigned the trivial name of rhinoquinone C to this novel homodimeric naphthoquinone.

Table 6. ^{1}H (400 MHz) and ^{13}C (100 MHz) NMR Data for Compound **6**, Recorded in $CDCl_3$.

Position	δ_C	Type	δ_H	Mult, *J* (Hz)
1	183.7	C		
2	141.6	C		
3	148.2	C		
4	187.2	C		
4a	109.6	C		
5	164.3	C		
6	106.3	CH	6.65	d, 2.5
7	165.8	C		
8	107.6	CH	7.14	d, 2.5
8a	133.5	C		
9	41.8	CH_2	3.72	s
10	203.1	C		
11	29.9	CH_3	2.06	s
12	19.9	CH_2	4.01	s
5-OH				
7-OCH_3	56.1	CH_3	3.89	s
1’	183.3	C		
2’	141.1	C		
3’	146.0	C		
4’	188.8	C		
4a’	110.1	C		
5’	160.5	C		
6’	120.1	C		
7’	163.1	C		
8’	102.9	CH	7.13	s
8a’	131.7	C		
9’	41.8	CH_2	3.76	s
10’	203.4	C		
11’	30.5	CH_3	2.31	s
12’	12.9	CH_3	2.09	s
5’-OH				
7’-OCH_3	56.5	CH_3	3.85	s

Compound **7** was isolated as a yellow amorphous solid. Its molecular formula was determined as $C_{30}H_{23}NO_9$ on the basis of the HRESIMS data ($[M+H]^+$ *m/z* = 542.1436, calculated *m/z* = 542.1446 for $C_{30}H_{24}NO_9$, Δ -1.8 ppm) with twenty degrees of

unsaturation. Similar to **6**, the ^{1}H spectrum shows remarkable similarities to two compounds, rhinoquinone A (**2**) and 6-deoxybostrycoidin (**4**), and almost appears as a 1:1 mixture of the two. However, like compound **6**, the C-12 methyl signal of **2** was absent, along with the H-6' signal being a singlet instead of a doublet as seen in the monomer (**4**) and a methylene unit with a similar shift to **6** (δ_H/δ_C 4.07 (s)/20.1) was present (**Figure 5**). The six key HMBC correlations for H_2-12 that were seen in **6** were also observed for compound **7** (**Figure 6**). The structure was elucidated primarily from the presence of the H_2-12 HMBC correlations and alignment of the monomer's and dimer's ^{1}H-NMR. Further analysis of the edited-HSQC and HMBC data confirmed the heterodimeric structure depicted in **Figure 2** and has been assigned the trivial name of rhinoquinone D (**7**).

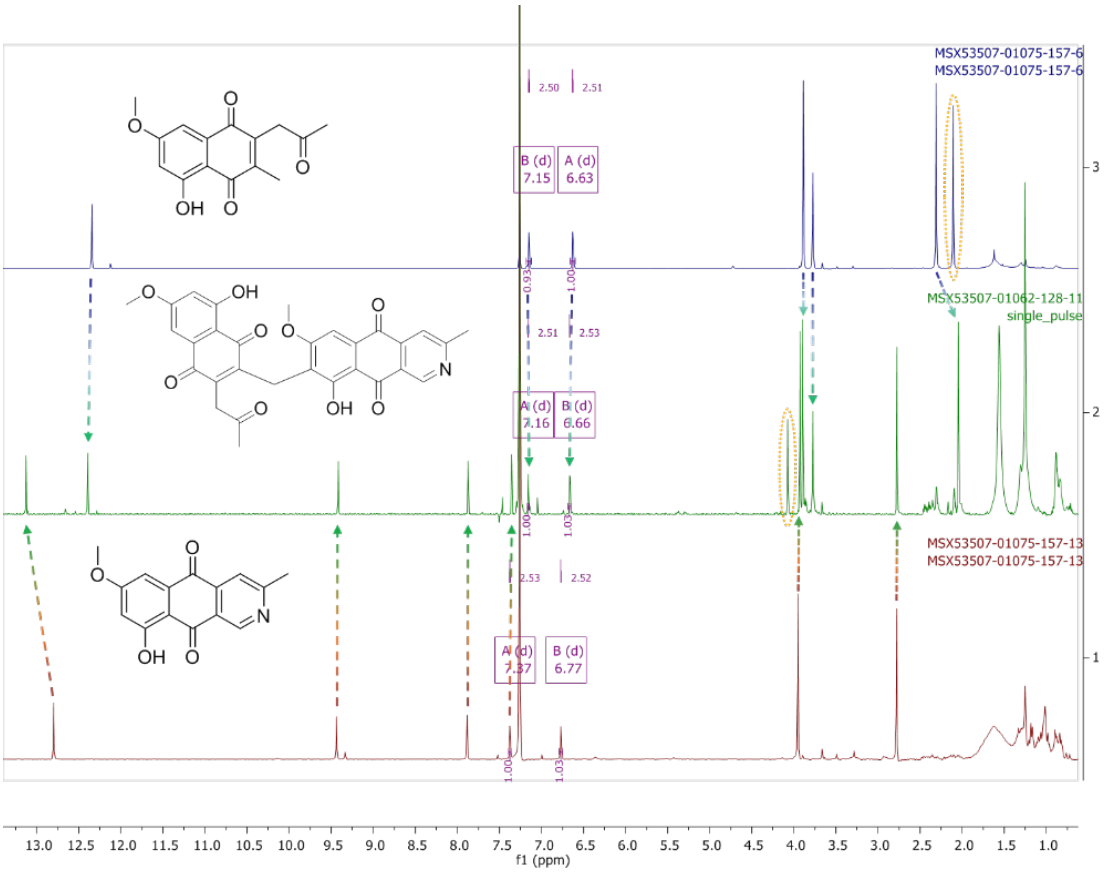

Figure 5. ^{1}H-NMR of Compounds **2**, **4**, and **7**, Showing Alignment of Peaks.

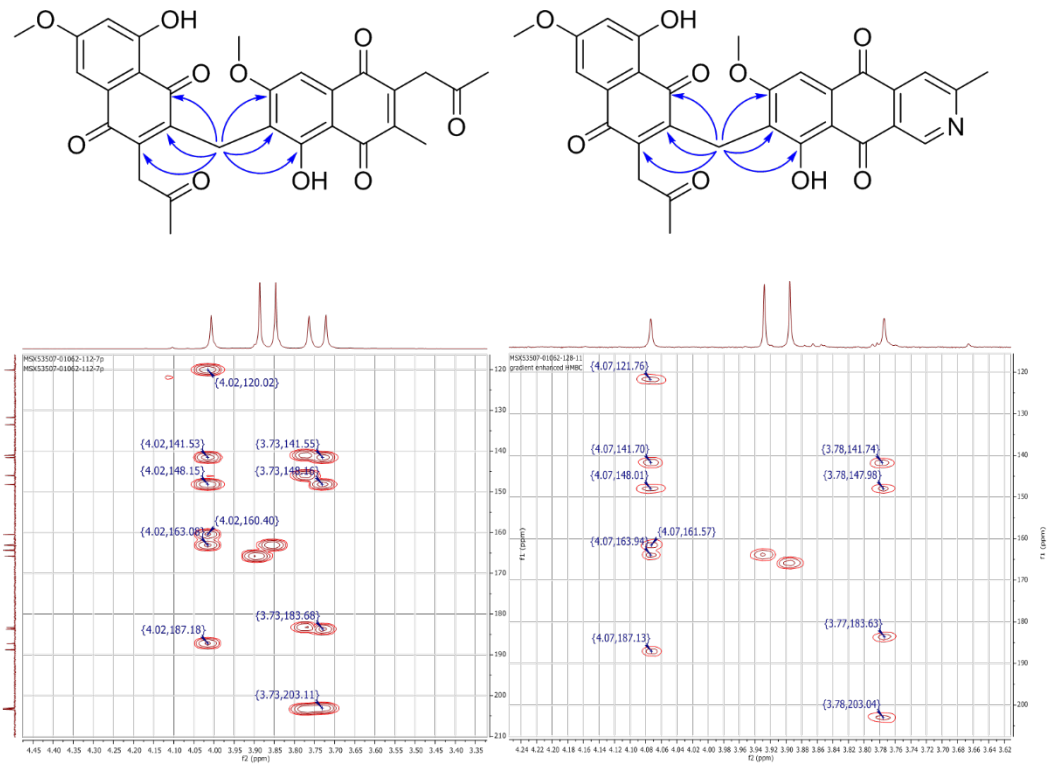

Figure 6. Key H_2-12 HMBC Correlations for Compounds **6** and **7**.

Biological Activity

Screening of initial fractions for cytotoxicity against breast cancer (MDA-MB-231), ovarian cancer (OVCAR3) and melanoma (MDA-MB-435) provided good preliminary cytotoxic activity (**Table 7**). Compounds **2-5** were isolated from fraction 5, while compound **6** was isolated from fraction 7.

Table 7. Preliminary Screening of Fractions for Cytotoxicity, Measured by Cell Viability.

Fraction	MDA-MB-231		OVCAR3		MDA-MB-435	
	20 µg/mL	2 µg/mL	20 µg/mL	2 µg/mL	20 µg/mL	2 µg/mL
5	28	59	17	84	9	14
7	44	99	66	85	10	59

At the recommendation of one of our collaborators, compounds **2**, **5** and **6** were tested against gram positive bacteria. He indicated previous work on structurally similar compounds were highly active against gram positive bacteria. Compounds **2** and **5** exhibited the best activity against *Staphylococcus aureus* (ATCC 35667) and a clinically relevant methicillin-resistant *S. aureus* strain (MRSA). The minimum inhibitory concentrations (MICs) of **2** and **5** against *S. aureus* were 6.3 μg/mL and 2.3 μg/mL and against MRSA were 19.4 μg/mL 16.0 μg/mL, respectively

Table 8. Minimum Inhibitory Concentrations (MIC) Needed for 100% Inhibition of Bacterial Growth for *S. aureus* and Methicillin Resistant *S. aureus* (MRSA).

Compound	MIC (μg/mL)	
	S. aureus	MRSA
2	6.3	19.4
5	2.3	16.0
6	68.8	452.2
Gentamicin	0.4	9.8

CHAPTER III

METHODOLOGY

General Experimental Procedures and Instrumentation

NMR data was obtained using either a JEOL ECS-400 NMR spectrometer equipped with a JEOL normal geometry broadband Royal probe and an autosampler (24-slots) operating at 400 MHz for ^{1}H and 100 MHz for ^{13}C, a JOEL ECA-500 NMR spectrometer operating at 500 MHz for ^{1}H and 125 MHz for ^{13}C (Both from JOEL Ltd.) or an Agilent 700 MHz NMR spectrometer equipped with a cryoprobe, operating at 700 MHz for ^{1}H and 175 MHz for ^{13}C (Agilent Technologies). HRESIMS data was collected with a Thermo QExactive Plus mass spectrometer coupled with an electrospray ionization source (ThermoFisher Scientific) coupled with a Waters Acquity UPLC system equipped with an Acquity BEH C_{18} column (1.7 μm; 50 mm x 2.1 mm) (Waters Corp.) and analyzed using the software Xcalibur (ThermoFisher Scientific). Phenomenex Gemini-NX C_{18} analytical (5 µm; 250 x 4.6 mm), semipreparative (5 µm; 250 x 10.0 mm), preparative (5 µm; 250 x 21.2 mm), Luna PFP preparative (5 µm; 250 x 19.0 mm), Luna Cyano analytical (5 µm; 250 x 4.6 mm) and Luna Cyano preparative (5 µm; 250 x 21.2 mm) columns (all from Phenomenex) were used on a Varian Prostar HPLC system equipped with Prostar 210 pumps and a Prostar 335 Photodiode array detector (PDA), with Galaxie Chromatography Workstation software (version 1.9.3.2, Varian Inc.) used for data collection and analysis. Flash chromatography was conducted on a Teledyne

ISCO CombiFlash Rf 200 system using Silica Gold columns (both from Teledyne Isco) and coupled with UV and evaporative light-scattering detectors. All other reagents and solvents were obtained from Fisher Scientific and VWR and were used without further purification.

Fungal Growth and Identification

Fungal strain MSX53507 was provided by our collaborator Mycosynthetix, and is a morphologically diverse fungus. This was observed when a total of ten cultures were examined and shown in **Figure 7**. The ITSrDNA was sequenced and analyzed with 21 taxa from several type strains of *Cladorrhinum* spp. (**Figure 8**). Due to the morphological diversity, this was performed for a total of 6 samples: two from the light region of the fungus, two from the dark region, and two from the junction where the light and dark intersect to confirm the observed morphologies were not due to a contamination or co-culture situation. Protocols for DNA extraction, PCR, Sanger sequencing, and phylogenetic analysis have been reviewed. Further work would need to be done to determine if fungal strain MSX53507 is a new species of *Cladorrhinum*, but the independent branching observed in the phylogenetic tree does confirm that is a new strain of *Cladorrhinum* sp..[41]

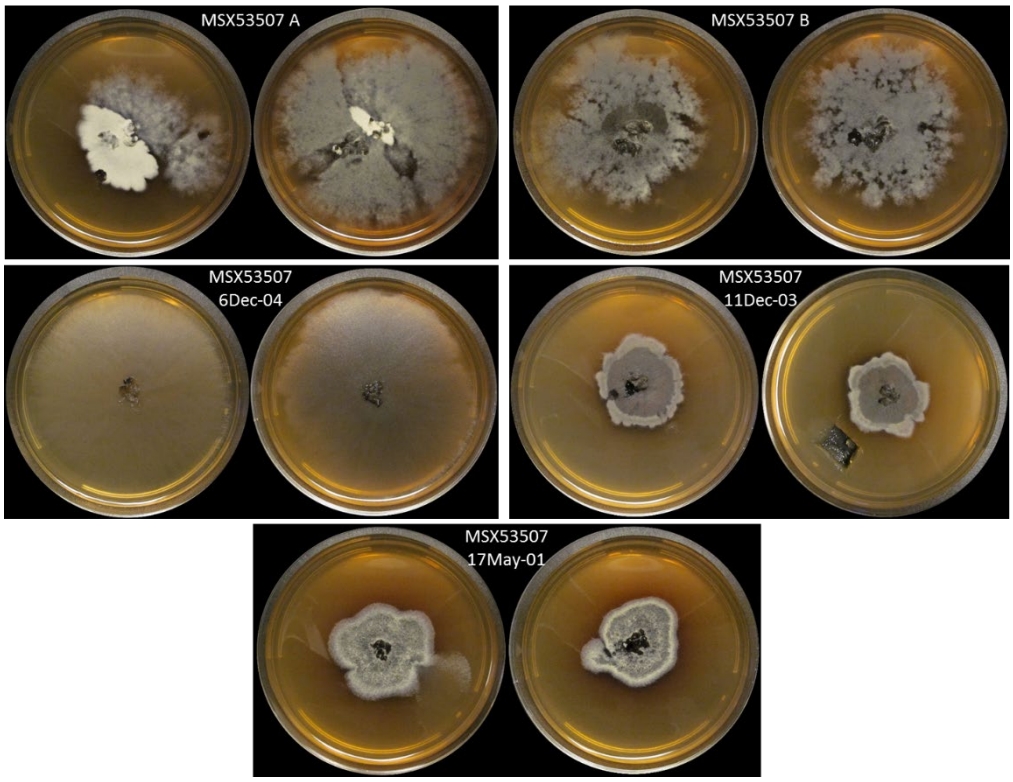

Figure 7. Depiction of the Observed Morphological Diversity of MSX53507.

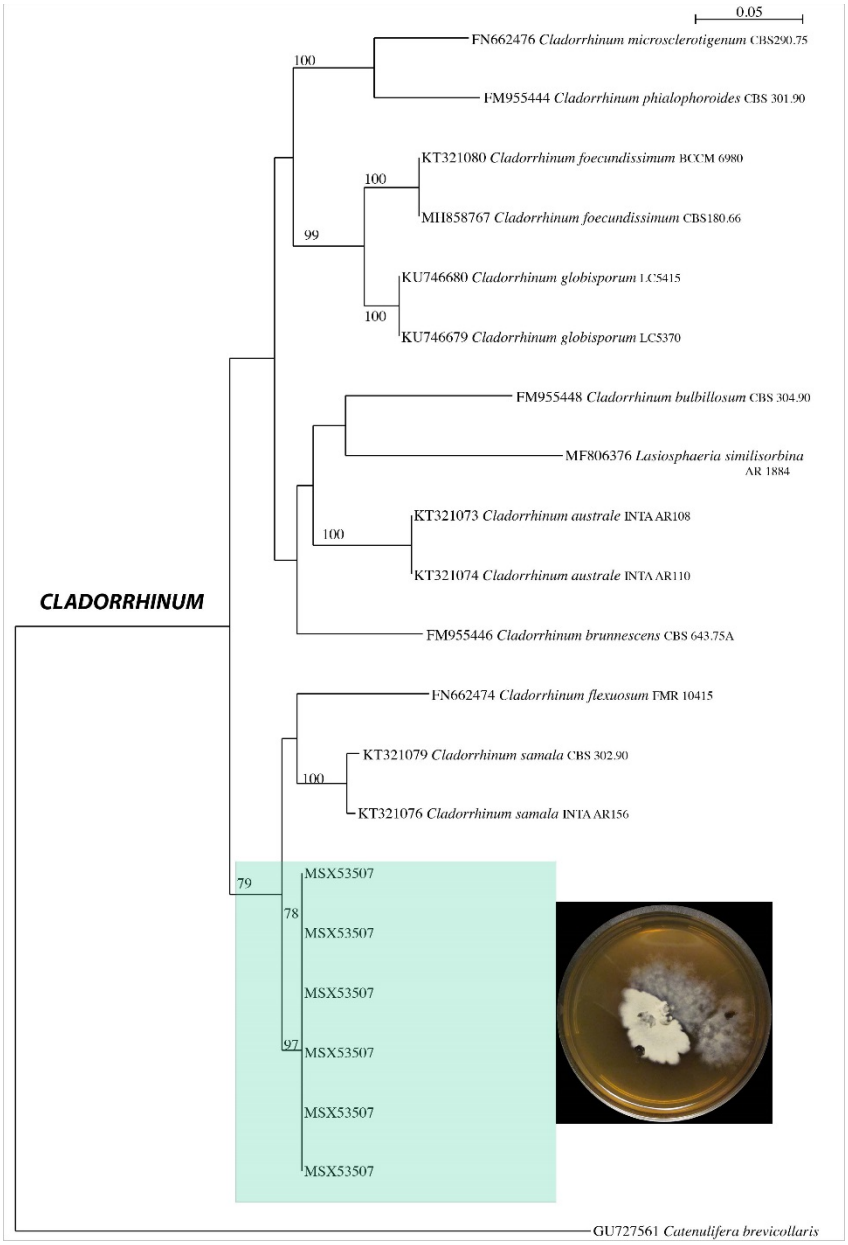

Figure 8. Phylogram of the Most Likely Tree (-lnL = 2549.85) from a RAxML Analysis of 21 Taxa Based on ITSrDNA Sequences (557 bp) from Several Type Strains of *Cladorrhinum* spp.. Numbers refer to the RAxML bootstrap support values ≥ 70% based on 1,000 replicates. Strain MSX53507 was identified as *Cladorrhinum* sp. (highlighted in green box). Several isolates of the same strain MSX53507 were sequenced since the cultural morphology varied between different isolates of the same strain. *Catenulifera brevicollaris* (GU727561) was used as outgroup. Bar indicates nucleotide substitutions per site.

Fermentation, Extraction and Isolation

Cultures of strain MSX53507 were grown in a Petri dish containing potato dextrose agar (PDA). Once sufficient mycelial growth was observed, a small agar plug with fungal mycelium was transferred to YESD (2% soy peptone, 2% dextrose, and 1% yeast extract). These seed cultures were grown and used as the inoculum. Cultures of strain MSX53507 were grown in three separate 2.8 L Fernbach flasks (Corning, Inc., Corning, NY, USA), with each containing 150 g rice and 300 mL H_2O and allowed to incubate for approximately four weeks. The light culture (1) was extracted independently, while the two dark solid cultures were extracted together. A total of 500 mL of 1:1 MeOH-$CHCl_3$ was added to each of the solid cultures, and they were chopped into small pieces with a spatula. They were then shaken at ~125 rpm overnight (~16 h) at room temperature and filtered under vacuum. This process was then repeated two more times for each extract. A total of 900 mL $CHCl_3$ and 1500 mL H_2O were added to each filtrate. The biphasic solution was stirred for 30 min and then transferred into a separatory funnel. The organic layer was drawn off and evaporated to dryness under reduced pressure. The dried organic extracts were re-constituted in 600 mL of 1:1 MeOH-CH_3CN and 600 mL of hexanes, and transferred to a separatory funnel. The MeOH-CH_3CN layer was drawn off and evaporated to dryness in vacuum. The defatted organic extracts of the light solid culture (~1.5 g) and the dark solid cultures (~4.1 g) were dissolved in $CHCl_3$, adsorbed onto Celite 545 and fractioned by flash chromatography. The light culture was fractioned via a 40 g RediSep Rf Gold HP Silica column using a gradient solvent system of hexane-$CHCl_3$-MeOH with a 40 mL/min flow rate and 53.3 column volumes over 63.9 min to

yield 19 fractions (L:F1-L:F19). The dark cultures were fractioned via a 80 g RediSep Rf Gold HP Silica column using a gradient solvent system of hexane-$CHCl_3$-MeOH with a 60 mL/min flow rate and 25.1 column volumes over 52.3 min to afford 23 fractions (D:F1-D:F23). Fraction L:F8 (~26.5 mg) was subjected to preparative HPLC using a gradient system of 35:65 to 55:45 CH_3CN-H_2O (0.1% formic acid) over 12 min then 70:30 to 100:0 CH_3CN-H_2O (0.1% formic acid) over 20 min at a flow rate of 21.20 mL/min and a Gemini column to yield compound **1** (1.0 mg, t_R 10.5 min). Fraction D:F11 (~40.0 mg) was subjected to preparative HPLC using the same gradient system of 35:65 to 55:45 CH_3CN-H_2O (0.1% formic acid) over 12 min then 70:30 to 100:0 CH_3CN-H_2O (0.1% formic acid) over 20 min at a flow rate of 21.20 mL/min and a Gemini column to yield compound **7** (1.2 mg, t_R 21.5 min). Fraction D:F10 (~1.0 g) was dissolved in $CHCl_3$, adsorbed onto Celite 545. It was fractionated by flash chromatography via a 12 g RediSep Rf Gold HP Silica column using a gradient solvent system of hexane-EtOAc-MeOH with a 30 mL/min flow rate and 38.9 column volumes over 21.8 min to yield 10 fractions (D:$F10_I$-D:$F10_X$). Fraction D:$F10_{VII}$ (~22.6 mg) was purified via solubility properties by adding MeOH to the sample, vortexing and then centrifuging the sample. The supernatant was removed and this process was repeated several times. The resulting precipitate yielded compound **6** (~11.4 mg). Fraction D:$F10_V$ (~76.2 mg) was subjected to preparative HPLC using a gradient system of 70:30 to 100:0 MeOH-H_2O (0.1% formic acid) over 30 min at a flow rate of 20.00 mL/min and a Luna PFP column to yield 13 subfractions (D:$F10_{V1}$-D:$F10_{V13}$). Fraction D:$F10_{V5}$ (~7.8 mg) was purified with preparative HPLC using a gradient system of 10:90 to 50:50 CH_3CN-H_2O (0.1% formic

acid) over 30 min at a flow rate of 21.20 mL/min and a Luna Cyano column to yield compound **5** (4.6 mg, t_R 19.0-21.0 min). Fraction D:F10$_{V6}$ (~5.7 mg) was purified with preparative HPLC using a gradient system of 10:90 to 50:50 CH_3CN-H_2O (0.1% formic acid) over 30 min at a flow rate of 21.20 mL/min and a Luna Cyano column to yield compound **2** (4.0 mg, t_R 24.0-25.0 min). Fraction D:F10$_{V7}$ (~5.6 mg) was purified with semi-preparative HPLC using a gradient system of 55:45 to 100:0 MeOH-H_2O (0.1% formic acid) over 30 min at a flow rate of 4.60 mL/min and a Gemini column to yield compound **3** (2.4 mg, t_R 17.0 min). D:F10$_{V13}$ (1.3 mg) was purified with analytical HPLC using a gradient system of 30:70 to 60:40 CH_3CN-H_2O (0.1% formic acid) over 30 min at a flow rate of 1.00 mL/min and a Luna Cyano column to yield compound **4** (0.8 mg, t_R 11.5 min). Compounds **3** and **7** were further purified by analytical HPLC to generate materials of a higher purity, while all other isolated compounds were at a suitable purity for biological evaluation. The purity of compounds for bioassays was determined by ^{1}H NMR.

X-Ray Crystallographic Analysis of Compound 2

Crystals of compound **2** formed from an approximate 1:1 mixture of MeOH and chloroform under nitrogen drying lines at room temperature. A brief summary of the previously described method, instrumentation and the computing details are as follows: Data collection: X8 Proteum-R (Bruker Analytical X-ray Instruments Inc., Madison, Wisconsin, USA); cell refinement: SAINT V8.38A (Bruker Analytical X-ray Instruments Inc., Madison, Wisconsin, USA); data reduction: SAINT V8.38A (Bruker Analytical

X-ray Instruments Inc., Madison, Wisconsin, USA); program(s) used to solve structure: ShelXT; program(s) used to refine structure: SHELXL; molecular graphics: Olex2 (Dolomanov et al., 2009); software used to prepare material for publication: Olex2. publCIF is used for generating the crystallographic information file (CIF).[42]

Biological Assays

Cytotoxicity – Cell Viability Assays

A previously described methodology was used for the cytotoxicity assays.[42, 43] In brief, all three cell lines, MDA-MB-435, MDA-MB-231, and OVCAR3 were purchased from American Type Culture Collection (Manassas, VA). The cells were grown under a set of specific conditions, and harvested when they were in their log phase of growth. A total of 5,000 cells were seeded per well (96-well plate) and incubated overnight. Samples to be tested were then dissolved in DMSO and added to the appropriate wells (concentrations: 20 μg/mL and 2 μg/mL). The cells were then incubated for 72 hours at 37°C and evaluated for cell viability with a commercial absorbance assay. The data are expressed as the percentage of cell survival relative to the solvent, DMSO (used as the control.)

Antibacterial - Minimum Inhibitory Concentration (MIC) Assays

Antibacterial activity of compounds **2**, **5** and **6** was assessed using a microdilution assays, monitoring growth inhibition against *Staphylococcus aureus* ATCC 35667 and a clinically relevant methicillin-resistant *S. aureus* strain (MRSA), at OD_{600}.[44] The Minimum Inhibitory Concentration (MIC) of each compound was carried out following

the Clinical and Laboratory Standards Institute (CLSI) guidelines.[45] In the MIC assays, 10 µL of log-phase bacteria, diluted at 5.0×10^6 colony forming units per milliliter (CFU/mL) were added to a 96 well plate. Compounds **2**, **5**, and **6** were evaluated at concentrations ranging from 0-200 µg/mL or 0-1000 µg/mL for gentamicin, in Müeller-Hinton broth (MHB) containing 2% DMSO, in a final volume of 100 µL. 96-Well plates were incubated at 37°C for 18 hours, after which OD_{600} values were measured using a Multiskan™ FC microplate reader (ThermoScientific) to evaluate growth inhibition. The MIC is defined as the lowest compound concentration at which growth is ≥95 % inhibited after 18−24 h of incubation at 37 °C. The MIC was calculated by nonlinear regression using a modified Gompertz equation (**Equation 1**), which relates the fractional area (y) to the log of antibacterial concentration (x).

$$y = A + Ce^{-e^{B(x-M)}} \quad \textbf{Equation 1}$$

Where A is the lower asymptote, B is a slope parameter, C is the distance between the lower and higher asymptote and M is the log concentration at the inflection point. The MIC (**Equation 2**) is defined as the intersection of line $y = A$ with the equation of the line tangential to the point $(M, (A + Ce^{-1}))$.[46] The values of A, C, B and M were obtained from nonlinear fitting using Prism 6.0.

$$MIC = 10^{\left(M+\frac{1}{B}\right)} \quad \textbf{Equation 2}$$

CHAPTER IV

CONCLUSIONS

In summary, preliminary cytotoxicity data for fungal strain MSX53507, in combination with results from an established dereplication protocol, indicated that the biological activity of MSX53507 was not attributable to any compounds (new or known) previously isolated and identified in our research laboratory. Thus, further investigation into the profile of secondary metabolites and isolation and elucidation of the compound(s) responsible for the bioactivity was warranted and three large scale cultures were ordered from our collaborator. They were extracted using an established methodology adapted in our laboratory for fungal cultures grown on solid media (rice) and the organic extract was then fractionated using flash chromatography. The obtained fractions were screened against a panel of three cancer cell lines, MDA-MB-435 (melanoma), MDA-MB-231 (breast), and OVCAR3 (ovarian). The cytotoxicity results allowed for further prioritization of fractions. A combination of two fractionation methodologies, bioactivity-guided and proton-NMR guided, led to the isolation and elucidation of four new naphthoquinone analogues (**1**, **3**, and **6-7**), two known compounds (**4-5**) and a naphthoquinone previously misidentified in the literature (**2**) from fractions that exhibited biological activity. The structures of the isolated compounds were established using a set of spectroscopic and spectrometric techniques. While genetic sequencing data determined that fungal strain MSX53507 is at least a new strain of

Cladorrhinum sp. and branches alone in the phylogenetic tree, additional work would need to be conducted to determine if is in fact a new species.

Compound **1** contains a bridged eight-member oxocine-one ring system in which the bridge creates two six-membered rings. To the best of my knowledge, is the first report of an oxocine-one core formed from a monomeric unit that has been isolated from fungi and was named Cladoxocinone A. In correction of the literature, this is the first report of both the spectroscopic and X-Ray crystallography data for compound **2**; establishing this as a new compound and named rhinoquinone A. The only difference between Rhinoquinone B (**3**) and compound **2** is a reduction of the ketone in the acetonyl chain to a hydroxy moiety. Even though there was some minor differences observed when comparing the spectroscopic data to that in the literature of both of the known compounds, 6-deoxybostrycoidin (**4**) and 6-deoxyfusarubin (**5**), the data was mostly in agreement and also aligned with the calculated and predicted ^{13}C NMR data (ACD laboratories NMR predictor software) for confirmation of the structures. Interestingly, while **1-5** are all monomeric 15-carbon containing compounds, **6** and **7** are an unprecedented, dimeric, 6'-12 head-to-tail binding of some of the isolated monomeric naphthoquinones. The first of these C-30 containing compounds, rhinoquinone C (**6**), contains two units of compound **2** and is considered to be a homodimer, while rhinoquinone D (**7**) is a heterodimer and contains one unit of compound **2** and one unit of 6-deoxybostrycoidin (**4**). Interestingly, this fungus's utilization of the same building blocks to generate some of the new chemotypes identified, ultimately showcases the broad and divergent biosynthetic pathways of fungi.

Preliminary cytotoxicity screening data of a fraction containing ~70% of compound **6** was observed to give a 10% survival rate for MDA-MB-435 at a 20 μg/mL concentration of the fraction, implying that compound **6** may have promising activity. Due to naphthoquinone's broad spectrum of biological activity, compounds **2**, **5**, and **6** were tested against *Staphylococcus aureus* (ATCC 35667) and a clinically relevant methicillin-resistant *S. aureus* strain (MRSA). Compound **5** was the most active with minimum inhibitory concentrations (MICs) of 2.3 μg/mL and 16.0 μg/mL, respectively.

REFERENCES

1. Society, A. C. Global Cancer Facts & Figures. https://www.cancer.org/research/cancer-facts-statistics/global.html (March 28),
2. (WHO), W. H. O., The Top 10 Causes of Death. **2018**.
3. Rodrigo-Troyano, A.; Sibila, O., The respiratory threat posed by multidrug resistant Gram-negative bacteria. *Respirology* **2017,** *22*, 1288-1299.
4. He, X.; Xie, M.; Li, S.; Ye, J.; Peng, Q.; Ma, Q.; Lu, X.; Zhong, B., Antimicrobial resistance in bacterial pathogens among hospitalized children with community acquired lower respiratory tract infections in Dongguan, China (2011–2016). *BMC Infectious Diseases* **2017,** *17*, 614.
5. Ahmed, S. M. A.-Z.; Abdelrahman, S. S.; Saad, D. M.; Osman, I. S.; Osman, M. G.; Khalil, E. A., Etiological trends and patterns of antimicrobial resistance in respiratory infections. *The open microbiology journal* **2018,** *12*, 34.
6. Newman, D. J.; Cragg, G. M., Natural Products as Sources of New Drugs from 1981 to 2014. *Journal of Natural Products* **2016,** *79*, 629-661.
7. Hawksworth, D. L.; Lücking, R., Fungal Diversity Revisited: 2.2 to 3.8 Million Species. *Microbiology Spectrum* **2017,** *5*.
8. Verpoorte, R., Exploration of nature's chemodiversity: the role of secondary metabolites as leads in drug development. *Drug Discovery Today* **1998,** *3*, 232-238.
9. Kinghorn, A. D.; De Blanco, E. J. C.; Lucas, D. M.; Rakotondraibe, H. L.; Orjala, J.; Soejarto, D. D.; Oberlies, N. H.; Pearce, C. J.; Wani, M. C.; Stockwell, B. R.; Burdette, J. E.; Swanson, S. M.; Fuchs, J. R.; Phelps, M. A.; Xu, L.; Zhang, X.; Shen, Y. Y., Discovery of Anticancer Agents of Diverse Natural Origin. *Anticancer Research* **2016,** *36*, 5623-5637.
10. Knowles, S. L.; Raja, H. A.; Wright, A. J.; Lee, A. M. L.; Caesar, L. K.; Cech, N. B.; Mead, M. E.; Steenwyk, J. L.; Ries, L. N. A.; Goldman, G. H.; Rokas, A.; Oberlies, N. H., Mapping the Fungal Battlefield: Using in situ Chemistry and Deletion Mutants to Monitor Interspecific Chemical Interactions Between Fungi. *Frontiers in Microbiology* **2019,** *10*.
11. Rivera-Chávez, J.; El-Elimat, T.; Gallagher, J. M.; Graf, T. N.; Fournier, J.; Panigrahi, G. K.; Deep, G.; Bunch, R. L.; Raja, H. A.; Oberlies, N. H., Delitpyrones: α-Pyrone Derivatives from a Freshwater Delitschia sp. *Planta medica* **2019,** *85*, 62-71.
12. Willis, K., State of the World's fungi 2018. *Royal Botanic Gardens, Kew* **2018**.
13. Barrera, V. A.; Martin, M. E.; Aulicino, M.; Martínez, S.; Chiessa, G.; Saparrat, M. C. N.; Gasoni, A. L., Carbon-substrate utilization profiles by Cladorrhinum (Ascomycota). *Revista Argentina de Microbiología* **2019**.
14. Carmarán, C. C.; Berretta, M.; Martínez, S.; Barrera, V.; Munaut, F.; Gasoni, L., Species diversity of Cladorrhinum in Argentina and description of a new species, Cladorrhinum australe. *Mycological Progress* **2015,** *14*, 94.

15. Madrid, H.; Cano, J.; Gené, J.; Guarro, J., Two new species of Cladorrhinum. *Mycologia* **2011,** *103*, 795-805.
16. Onodera, H.; Hasegawa, A.; Tsumagari, N.; Nakai, R.; Ogawa, T.; Kanda, Y., MPC1001 and Its Analogues: New Antitumor Agents from the Fungus Cladorrhinum Species. *Organic Letters* **2004,** *6*, 4101-4104.
17. Qiu, H.-Y.; Wang, P.-F.; Lin, H.-Y.; Tang, C.-Y.; Zhu, H.-L.; Yang, Y.-H., Naphthoquinones: A continuing source for discovery of therapeutic antineoplastic agents. *Chemical Biology & Drug Design* **2018,** *91*, 681-690.
18. Yang, Z.; Ding, J.; Ding, K.; Chen, D.; Cen, S.; Ge, M., Phomonaphthalenone A: A novel dihydronaphthalenone with anti-HIV activity from Phomopsis sp. HCCB04730. *Phytochemistry Letters* **2013,** *6*, 257-260.
19. Parisot, D.; Devys, M.; Barbier, M., 6-O-Demethyl-5-deoxyfusarubin and its anhydro derivative produced by a mutant of the fungus Nectria haematococca blocked in fusarubin biosynthesis. *The Journal of antibiotics* **1991,** *44*, 103-107.
20. Arnstein, H. R. V.; Cook, A. H., 189. Production of antibiotics by fungi. Part III. Javanicin. An antibacterial pigment from Fusarium javanicum. *Journal of the Chemical Society (Resumed)* **1947**, 1021-1028.
21. Khan, M. I. H.; Sohrab, M. H.; Rony, S. R.; Tareq, F. S.; Hasan, C. M.; Mazid, M. A., Cytotoxic and antibacterial naphthoquinones from an endophytic fungus, Cladosporium sp. *Toxicology Reports* **2016,** *3*, 861-865.
22. Chowdhury, N. S.; Sohrab, M. H.; Rana, M. S.; Hasan, C. M.; Jamshidi, S.; Rahman, K. M., Cytotoxic Naphthoquinone and Azaanthraquinone Derivatives from an Endophytic Fusarium solani. *Journal of Natural Products* **2017,** *80*, 1173-1177.
23. Shah, A.; Rather, M. A.; Hassan, Q. P.; Aga, M. A.; Mushtaq, S.; Shah, A. M.; Hussain, A.; Baba, S. A.; Ahmad, Z., Discovery of anti-microbial and anti-tubercular molecules from Fusarium solani: an endophyte of Glycyrrhiza glabra. *Journal of Applied Microbiology* **2017,** *122*, 1168-1176.
24. Khan, N.; Afroz, F.; Begum, M. N.; Roy Rony, S.; Sharmin, S.; Moni, F.; Mahmood Hasan, C.; Shaha, K.; Sohrab, M. H., Endophytic Fusarium solani: A rich source of cytotoxic and antimicrobial napthaquinone and aza-anthraquinone derivatives. *Toxicology Reports* **2018,** *5*, 970-976.
25. Zhou, Y.-H.; Zhang, M.; Zhu, R.-X.; Zhang, J.-Z.; Xie, F.; Li, X.-B.; Chang, W.-Q.; Wang, X.-N.; Zhao, Z.-T.; Lou, H.-X., Heptaketides from an Endolichenic Fungus Biatriospora sp. and Their Antifungal Activity. *Journal of Natural Products* **2016,** *79*, 2149-2157.
26. Stodůlková, E.; Man, P.; Kuzma, M.; Černý, J.; Císařová, I.; Kubátová, A.; Chudíčková, M.; Kolařík, M.; Flieger, M., A highly diverse spectrum of naphthoquinone derivatives produced by the endophytic fungus Biatriospora sp. CCF 4378. *Folia Microbiologica* **2015,** *60*, 259-267.
27. Kharwar, R. N.; Verma, V. C.; Kumar, A.; Gond, S. K.; Harper, J. K.; Hess, W. M.; Lobkovosky, E.; Ma, C.; Ren, Y.; Strobel, G. A., Javanicin, an Antibacterial Naphthaquinone from an Endophytic Fungus of Neem, Chloridium sp. *Current Microbiology* **2009,** *58*, 233-238.

28. Halicki, P. C. B.; Ferreira, L. A.; De Moura, K. C. G.; Carneiro, P. F.; Del Rio, K. P.; Carvalho, T. d. S. C.; Pinto, M. d. C. F. R.; da Silva, P. E. A.; Ramos, D. F., Naphthoquinone Derivatives as Scaffold to Develop New Drugs for Tuberculosis Treatment. *Frontiers in Microbiology* **2018,** *9*.
29. Sperry, J.; Lorenzo-Castrillejo, I.; Brimble, M. A.; Machín, F., Pyranonaphthoquinone derivatives of eleutherin, ventiloquinone L, thysanone and nanaomycin A possessing a diverse topoisomerase II inhibition and cytotoxicity spectrum. *Bioorganic & Medicinal Chemistry* **2009,** *17*, 7131-7137.
30. Naysmith, B. J.; Hume, P. A.; Sperry, J.; Brimble, M. A., Pyranonaphthoquinones – isolation, biology and synthesis: an update. *Natural Product Reports* **2017,** *34*, 25-61.
31. Higa, M.; Noha, N.; Yokaryo, H.; Ogihara, K.; Yogi, S., Three New Naphthoquinone Derivatives from Diospyros maritima B<small>LUME</small>. *Chemical and Pharmaceutical Bulletin* **2002,** *50*, 590-593.
32. El-Elimat, T.; Figueroa, M.; Ehrmann, B. M.; Cech, N. B.; Pearce, C. J.; Oberlies, N. H., High-resolution MS, MS/MS, and UV database of fungal secondary metabolites as a dereplication protocol for bioactive natural products. *J Nat Prod* **2013,** *76*, 1709-16.
33. Paguigan, N. D.; El-Elimat, T.; Kao, D.; Raja, H. A.; Pearce, C. J.; Oberlies, N. H., Enhanced dereplication of fungal cultures via use of mass defect filtering. *J Antibiot* **2017,** *70*, 553-561.
34. Li, H.-M.; Tang, Y.-L.; Zhang, Z.-H.; Liu, C.-J.; Li, H.-Z.; Li, R.-T.; Xia, X.-S., Compounds from Arnebia euchroma and their related anti-HCV and antibacterial activities. *Planta medica* **2012,** *78*, 39-45.
35. Barnes, E. C.; Jumpathong, J.; Lumyong, S.; Voigt, K.; Hertweck, C., Daldionin, an Unprecedented Binaphthyl Derivative, and Diverse Polyketide Congeners from a Fungal Orchid Endophyte. *Chemistry – A European Journal* **2016,** *22*, 4551-4555.
36. Parisot, D.; Devys, M.; Barbier, M., 6-O-demethyl-5-deoxybostrycoidin, A 2-aza-anthraquinone produced by the fungus Nectria haematococca. *Phytochemistry* **1990,** *29*, 3364-3365.
37. Bu-zhu, Y. U.; Cheng-zhi, S.; Zhi-zhi, D. U.; Xiang-hai, C. A. I.; Sheng-xiong, H.; Xiao-dong, L. U. O., Naphthaquinones from Fusarium sp. 1RGa-1b, an Endophytic Fungus Associated with Trewia nudiflora (Euphorbiaceae). *Natural Product Research & Development* **2009,** *21*, 574-576.
38. Tatum, J. H.; Baker, R. A., Naphthoquinones produced by Fusarium solani isolated from citrus. *Phytochemistry* **1983,** *22*, 543-547.
39. Parisot, D.; Devys, M.; Barbier, M., Notizen: 5-Deoxybostrycoidin, a New Metabolite Produced by the Fungus Nectria haematococca (Berk. and Br.) Wr. In *Zeitschrift für Naturforschung B*1989; Vol. 44, p 1473.
40. Parisot, D.; Devys, M.; Barbier, M., A new deoxyfusarubin produced by the fungus Nectria haematococca. *The Journal of antibiotics* **1992,** *45*, 1799-1801.
41. Raja, H. A.; Miller, A. N.; Pearce, C. J.; Oberlies, N. H., Fungal Identification Using Molecular Tools: A Primer for the Natural Products Research Community. *J Nat Prod* **2017,** *80*, 756-770.

42. El-Elimat, T.; Raja, H. A.; Ayers, S.; Kurina, S. J.; Burdette, J. E.; Mattes, Z.; Sabatelle, R.; Bacon, J. W.; Colby, A. H.; Grinstaff, M. W.; Pearce, C. J.; Oberlies, N. H., Meroterpenoids from Neosetophoma sp.: A Dioxa[4.3.3]propellane Ring System, Potent Cytotoxicity, and Prolific Expression. *Organic Letters* **2019,** *21*, 529-534.
43. Sica, V. P.; Rees, E. R.; Raja, H. A.; Rivera-Chávez, J.; Burdette, J. E.; Pearce, C. J.; Oberlies, N. H., In situ mass spectrometry monitoring of fungal cultures led to the identification of four peptaibols with a rare threonine residue. *Phytochemistry* **2017,** *143*, 45-53.
44. Rivera-Chávez, J.; Caesar, L. K.; Garcia-Salazar, J. J.; Raja, H. A.; Cech, N. B.; Pearce, C. J.; Oberlies, N. H., Mycopyranone: A 8,8ˈ-binaphthopyranone with potent anti-MRSA activity from the fungus Phialemoniopsis sp. *Tetrahedron Lett* **2019,** *60*, 594-597.
45. CLSI, Methods for Dilution Antimicrobial Sucseptibility Tests for Bacteria That Grow Aerobically. *Clinical and Laboratory Standards Institute* **2015,** *Approved Standard-Tenth Edition*, Wayne, PA.
46. Lambert, R. J.; Pearson, J., Susceptibility testing: accurate and reproducible minimum inhibitory concentration (MIC) and non-inhibitory concentration (NIC) values. *J Appl Microbiol* **2000,** *88*, 784-90.

APPENDIX A

SPECTRAL DATA

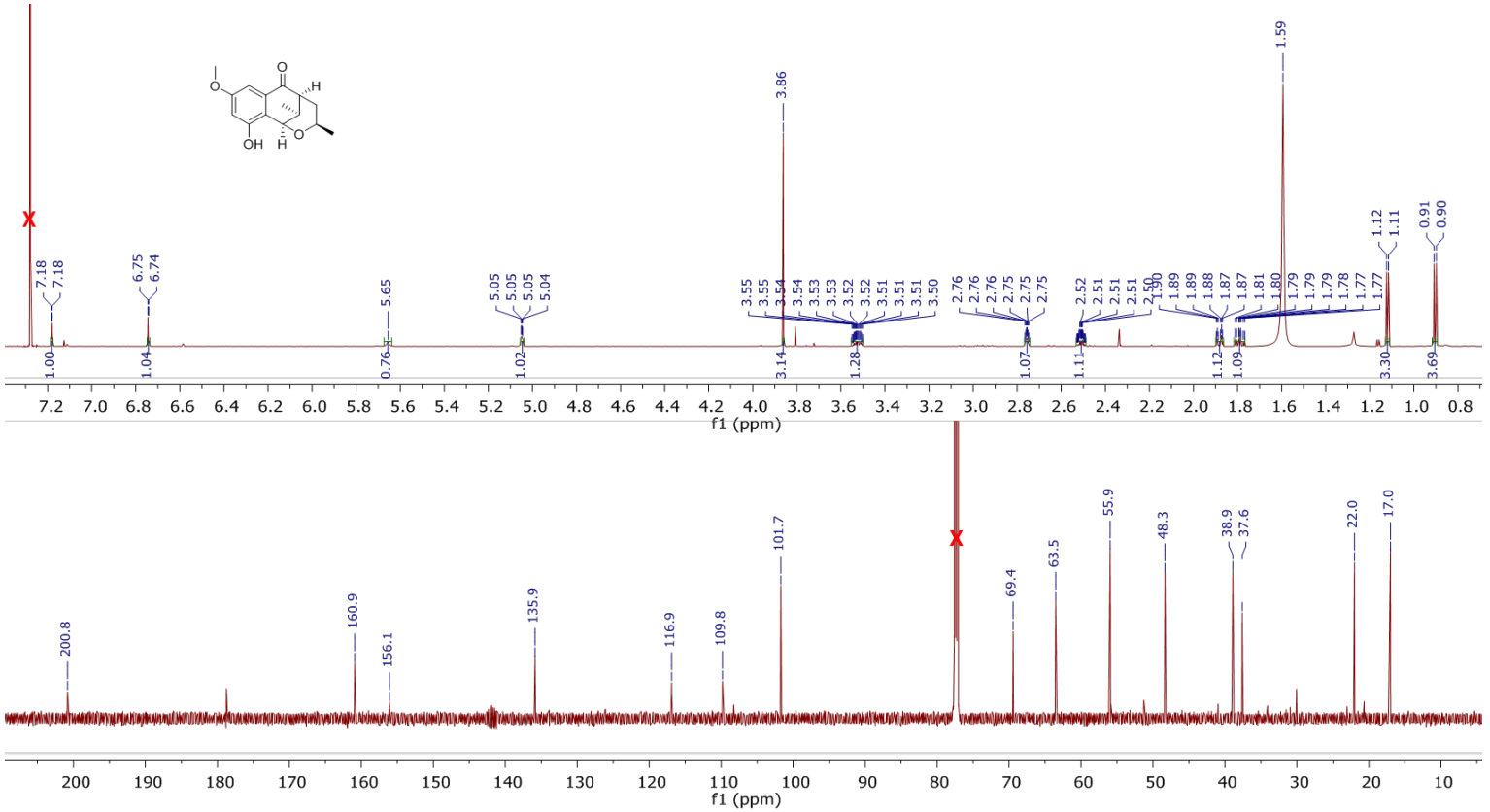

Figure A1. Top - ^{1}H-NMR Spectrum (700 MHz) and Bottom ^{13}C-NMR Spectrum (175 MHz) for Compound **1**, Recorded in $CDCl_3$.

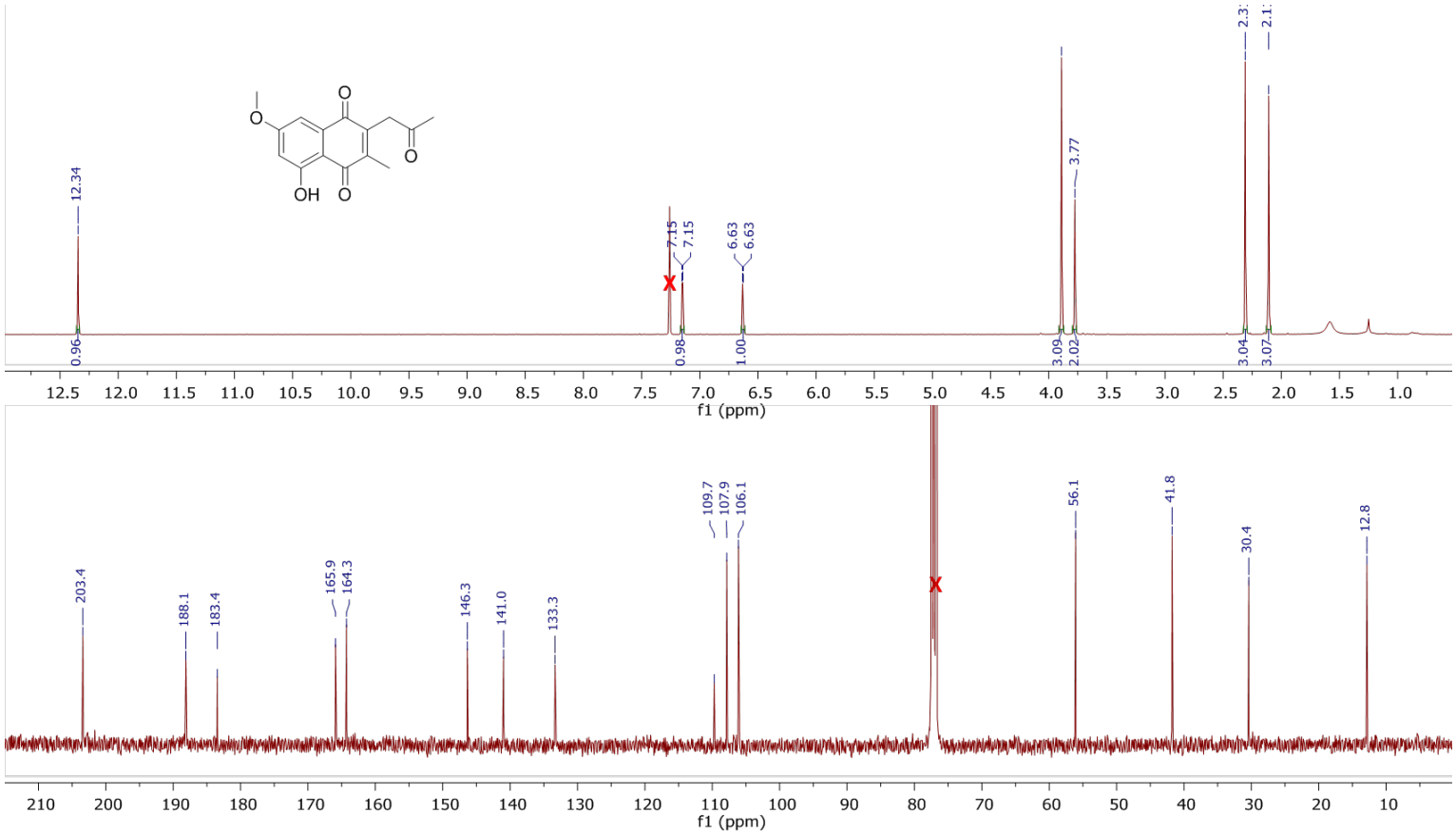

Figure A2. Top - ^{1}H-NMR Spectrum (400 MHz) and Bottom ^{13}C-NMR Spectrum (100 MHz) for Compound **2**, Recorded in $CDCl_3$.

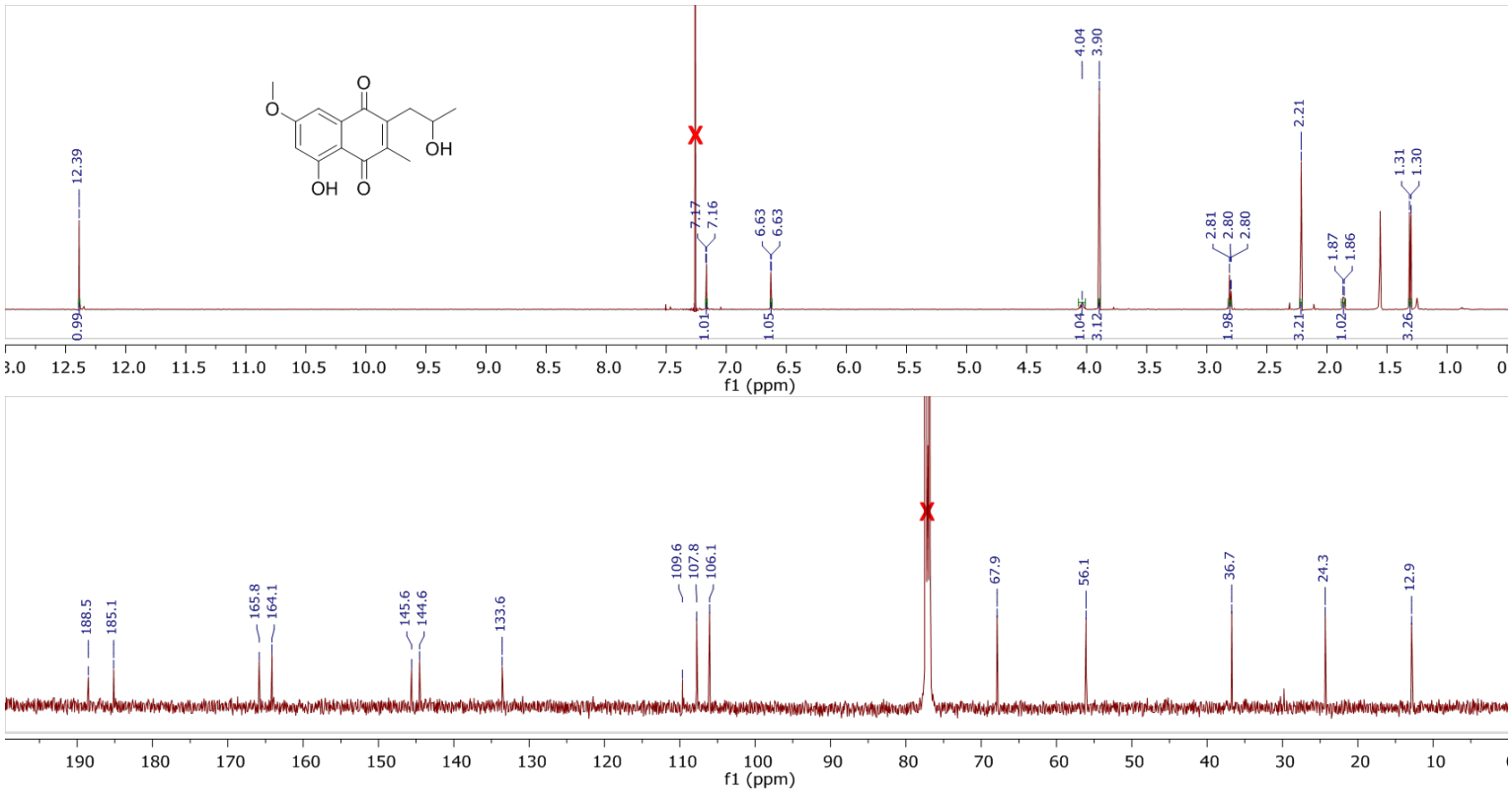

Figure A3. Top - ^{1}H-NMR Spectrum (500 MHz) and Bottom ^{13}C-NMR Spectrum (125 MHz) for Compound **3**, Recorded in $CDCl_3$.

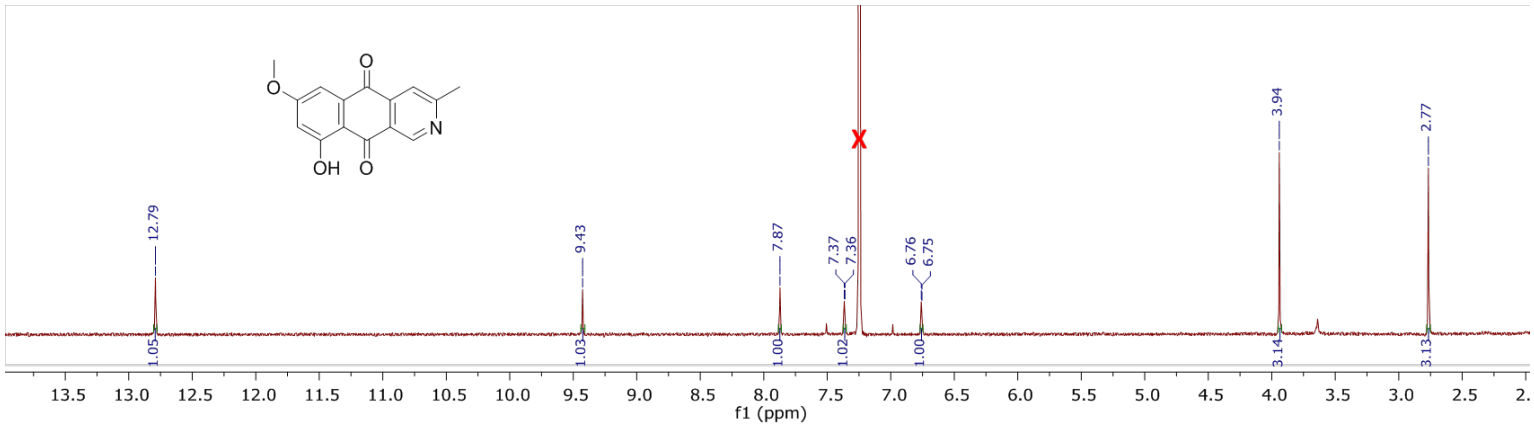

Figure A4. ^{1}H-NMR Spectrum (400 MHz) for Compound **4**, Recorded in $CDCl_3$.

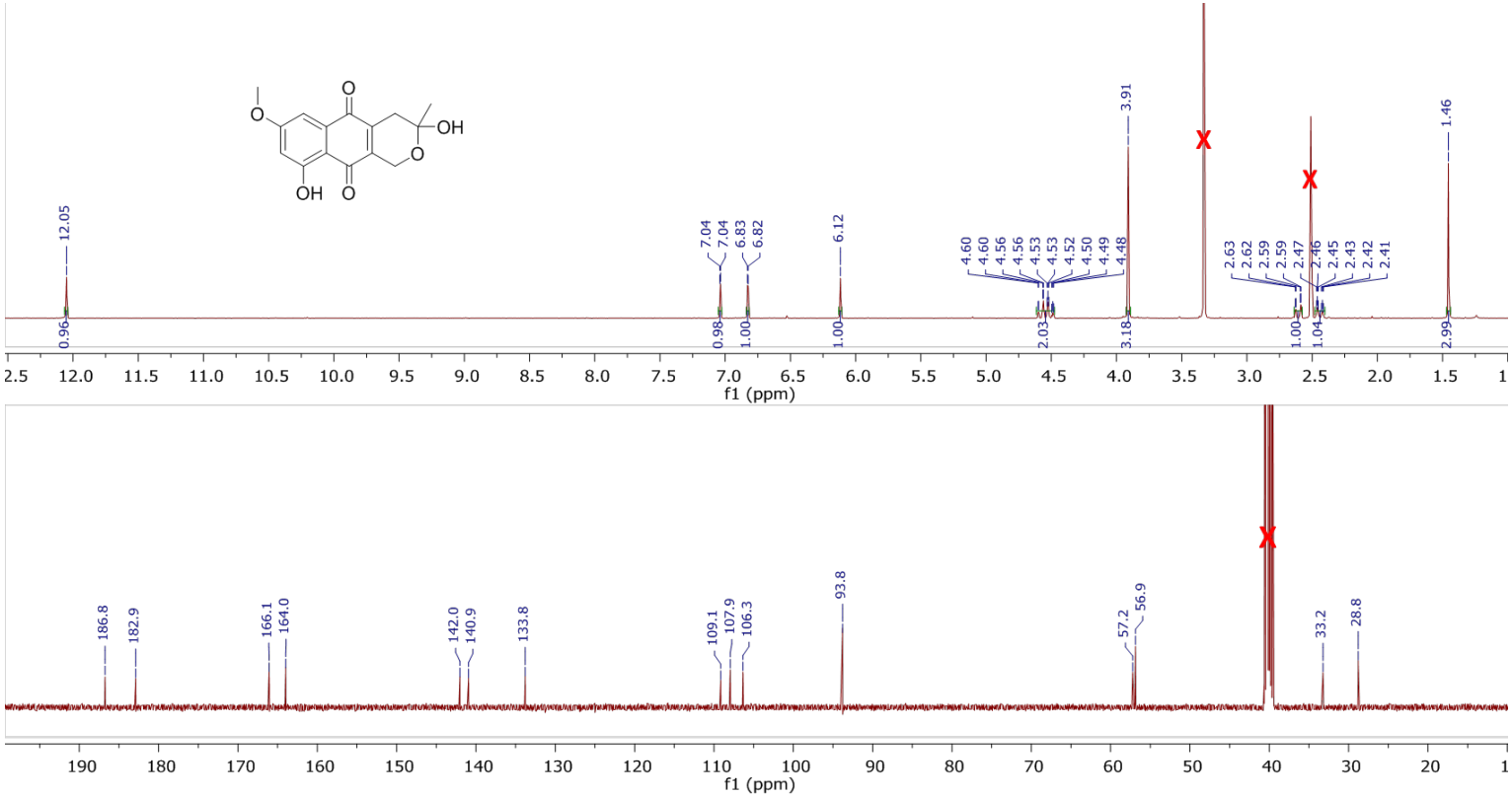

Figure A5. Top - ^{1}H-NMR Spectrum (500 MHz) and Bottom ^{13}C-NMR Spectrum (125 MHz) for Compound **5**, Recorded in $(CD_3)_2SO$.

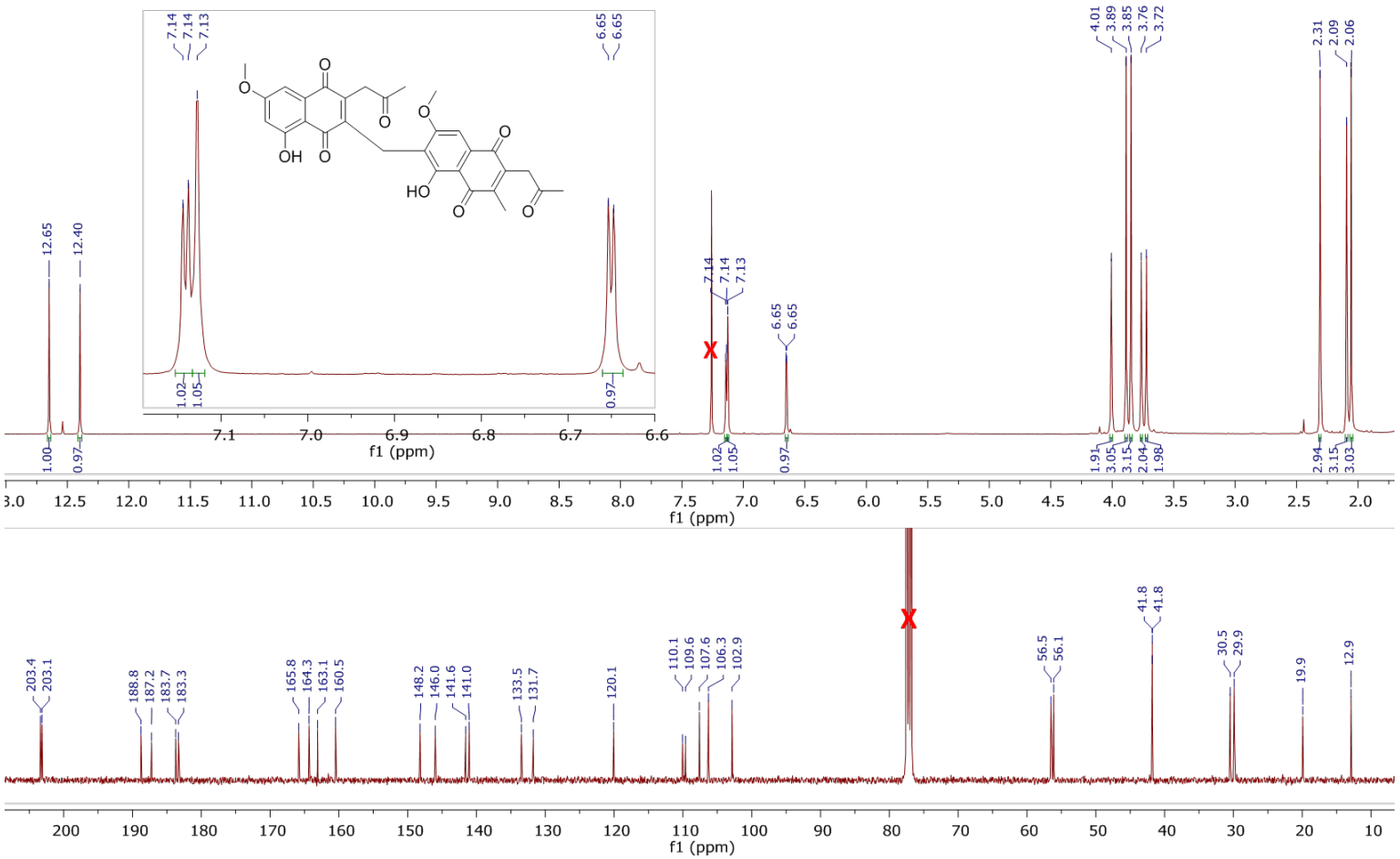

Figure A6. Top - ^{1}H-NMR Spectrum (400 MHz) and Bottom ^{13}C-NMR Spectrum (100 MHz) for Compound **6**, Recorded in $CDCl_3$.